

**SYNTHESIS AND SUPRAMOLECULAR STRUCTURE
OF COCRYSTALLINE CATECHOL AND HEXAMINE**

Kadsada Sala

**A Thesis Submitted in Partial Fulfillment of the Requirements for the
Degree of Master of Science in Chemistry
Suranaree University of Technology
Academic Year 2009**

การสังเคราะห์และโครงสร้างซูปราโมเลคิวลาร์ของผลิตภัณฑ์ระหว่างแคททีคอล
และเฮกซามีน

นางสาวเกศญา สาลา

วิทยานิพนธ์นี้เป็นส่วนหนึ่งของการศึกษาตามหลักสูตรปริญญาวิทยาศาสตรมหาบัณฑิต
สาขาวิชาเคมี
มหาวิทยาลัยเทคโนโลยีสุรนารี
ปีการศึกษา 2552

SYNTHESIS AND SUPRAMOLECULAR STRUCTURE OF COCRYSTALLINE CATECHOL AND HEXAMINE

Suranaree University of Technology has approved this thesis submitted in partial fulfillment of the requirements for a Master's Degree.

Thesis Examining Committee

(Assoc. Prof. Dr. Malee Tangsathitkulchai)

Chairperson

(Assoc. Prof. Dr. Kenneth J. Haller)

Member (Thesis Advisor)

(Asst. Prof. Dr. Kunwadee Rangsriwatananon)

Member

(Dr. Weenawan Somphon)

Member

(Prof. Dr. Sukit Limpijumnong)

Vice Rector for Academic Affairs

(Assoc. Prof. Dr. Prapun Manyum)

Dean of Institute of Science

เกษฎา สาตา : การสังเคราะห์และโครงสร้างซูปราโมเลคิวลาร์ของผลึกร่วมระหว่าง
แคททีคอลและเฮกซามีน (SYNTHESIS AND SUPRAMOLECULAR STRUCTURE
OF COCRYSTALLINE CATECHOL AND HEXAMINE) อาจารย์ที่ปรึกษา :
รองศาสตราจารย์ ดร. เค็นเนท เจ. แสเลอว์, 100 หน้า.

ผลึกร่วมอัตราส่วน 2:1 ของแคททีคอลและเฮกซามีน เตรียมโดยตกผลึกในสารละลายผสม
ระหว่างคลอโรฟอร์มและไดเอทิลอีเทอร์ และได้ทำการศึกษาโครงสร้างด้วยรังสีเอกซ์ผลึกเชิงเดี่ยว
พบว่าในโครเจนทุกระยะของเฮกซามีนมีส่วนร่วมในการเกิดพันธะไฮโดรเจนแบบแข็งแรงกับตัว
ให้ไฮโดรเจน O-H ของแคททีคอล เกิดเป็นวงแบบ $R_4^4(18)$ ซึ่งเชื่อมผ่านโมเลกุลของเฮกซามีนเกิด
เป็นโครงสร้างแบบสายโซ่ 1 มิติที่ประกอบด้วยโมเลกุลของแคททีคอลและเฮกซามีนสลับกันไป
หมู่ไฮดรอกซิล 1 หมู่ที่เกิดเป็นทั้งพันธะไฮโดรเจนแบบแข็งแรงภายในโมเลกุล ($d[\text{O}\cdots\text{O}] = 2.724$
(1) Å, 103.0 (16)°) และระหว่างโมเลกุล ($d[\text{O}\cdots\text{N}] = 2.822$ (1) Å, 160 (2)°) เกิดเป็นรูปแบบพันธะ
ไฮโดรเจนแบบสัญลักษณ์ $S(5)$ ส่วนหมู่ไฮดรอกซิลอีกหนึ่งหมู่มีส่วนร่วมทั้งในการรับพันธะ
ไฮโดรเจนแบบแข็งแรง ($d[\text{O}\cdots\text{N}] = 2.760$ (1) Å, 162 (2)°) และการให้พันธะไฮโดรเจนแบบอ่อน
($d[\text{C}\cdots\text{O}] = 3.026$ (1) Å, 111.4 (11)°) ส่วนพันธะไฮโดรเจนแบบอ่อนมีรูปแบบสัญลักษณ์ที่อธิบาย
อันตรกิริยาแบบ $R_2^2(8)$ พันธะไฮโดรเจนระหว่างโมเลกุล C-H $\cdots\pi$ แบบ edge-to-face ของวงฟีนิล
อยู่บนแกนหมุนเกลียว 2_1 (2_1 -screw) เกิดการเรียงตัวซ้อนกันเป็นแบบ herringbone column

KADSADA SALA : SYNTHESIS AND STRUCTURAL STUDIES OF
ORGANIC COCRYSTALLINE MATERIALS. THESIS ADVISOR :
ASSOC. PROF. KENNETH J. HALLER, Ph.D. 100 PP.

HYDROGEN BOND PATTERN/GRAPH SET ANALYSIS/COCRYSTAL/
MOLECULAR CRYSTAL

The 2:1 cocrystalline adduct of catechol and hexamine has been prepared by solution crystallization using mixed chloroform and diethyl ether as solvents, and studied using single crystal X-ray structure analysis. The strong N-atom hydrogen bond acceptors of hexamine all participate in hydrogen bonds with the strong O-H donors of catechol, forming local $R_4^4(18)$ rings, which link through the hexamine molecules to form one-dimensional chains of alternating catechol and hexamine molecules. One hydroxyl group participates in both intramolecular ($d[\text{O}\cdots\text{O}] = 2.724$ (1) Å, 103.0 (16)°) and intermolecular ($d[\text{O}\cdots\text{N}] = 2.822$ (1) Å, 160 (2)°) strong hydrogen bonds, creating hydrogen bonding motifs with graph theory designation $S(5)$. The other hydroxyl group participates in one strong donor ($d[\text{O}\cdots\text{N}] = 2.760$ (1) Å, 162 (2)°) and one weak hydrogen bond acceptor ($d[\text{C}\cdots\text{O}] = 3.026$ (1) Å, 111.4 (11)°) interactions. Including the weak hydrogen bond the graph set notation describing the intermolecular interactions would be designated $R_2^2(8)$. Intermolecular C-H $\cdots\pi$ edge-to-face hydrogen bond interactions of phenyl rings propagated by 2_1 -screw axes are also present as herringbone columns.

School of Chemistry

Student's Signature_____

Academic Year 2009

Advisor's Signature_____

ACKNOWLEDGEMENTS

First of all, I would like to express my gratitude to my supervisor, Assoc. Prof. Dr. Kenneth J. Haller, for his guidance and patience throughout the years of my study at Suranaree University of Technology. Not only has he taught me through, but also treated me to stronger and to take responsibility when I was getting stuck with problems. With his philosophy and psychology, he forces his students to present, to exchange and to discuss their ideas with other scientists not specific only chemist. Therefore, his vision, I had also been to foreign and beneficial my personal growth.

I would like to thank Assoc. Prof. Dr. Malee Tangsathitkulchai chairperson of my committee and Assist. Prof. Dr. Kulwadee Rangsriwathana for their invaluable contributions during my study at SUT, and for being members of my committee.

I would like to express special thanks to ex-members of our group, Dr. Weenawan Somphon at Kasetsart University, Kamphaengsaen Campus for being at thesis examiner and for discussions and suggestions in chemistry, Dr. Ratchadaporn Puntharod at Maejo University for her guidance, explanations and kindness, and especially to Dr. Kittipong Chainok at Rangsit University for his helpfulness, advice and guarantee during my studying and living in Korat.

I would like to thank all of our members of the Crystallography and Applied Surface Science Research Group, Suranaree University of Technology, especially Samroeng Krachodnok, Angkana Chatkon, Winya Dungkaew, Orrasa In-noi, Oratai Saisa-ard, Jittima Thisuwan, Monta Meepruek and Saiphon A. Kohnhorst

for their friendship, generous help, sharing knowledge, social activities, and companionship in the office and group meetings. They are fantastic. I would like to thank all of staffs at school of Chemistry, Suranaree University of Chemistry and the Center for Scientific and Technological Equipment for their assistance and suggestion for the use of XRD, FTIR, DTA/TGA and CHN/O.

I would like to thank my housemates (Thapanee Khumbudda and Sompong Saenseanya), my best friends for discussion and suggestions.

Last, but always greatest, I am extremely appreciative to my parents, my brother, and my sister for every support and encouragement throughout the long time of my study, and without whose love and understanding this work would not have been possible.

Kadsada Sala

CONTENTS

	Page
ABSTRACT IN THAI.....	I
ABSTRACT IN ENGLISH	II
ACKNOWLEDGEMENTS	III
CONTENTS.....	V
LIST OF TABLES	VIII
LIST OF FIGURES	IX
LIST OF ABBREVIATIONS.....	XI
 CHAPTER	
I INTRODUCTION.....	1
1.1 Crystallographic Background	1
1.2 Databases	3
1.3 Crystal Engineering.....	5
1.4 Supramolecular Interaction	7
1.5 Hydrogen Bonds	9
1.6 Cocrystals.....	14
1.7 Practical Techniques	17
II LITERATURE BACKGROUND.....	20
2.1 Hexamine Molecule	20
2.2 Cocrystallized Hexamine and Phenols.....	21

CONTENTS (Continued)

	Page
III EXPERIMENTAL	31
3.1 Materials	31
3.1.1 Chemical Reagents	31
3.1.2 Laboratory Materials	32
3.2 Equipments	32
3.2.1 Laboratory Equipment	32
3.2.2 Instrumentation	33
3.2.3 Databases	34
3.3 Procedures	34
3.3.1 Crystallization of Hexamine and Catechol.....	34
3.3.2 Structure Solution and Refinement	35
IV SUPRAMOLECULAR STRUCTURE OF COCRYSTALLINE	
CATECHOL AND HEXAMINE	37
4.1 Introduction	37
4.2 Materials and Methods	41
4.3 Results and Discussion.....	47
4.4 Conclusion	57
V SUMMARY AND CONCLUSION.....	58
REFERENCES	61

CONTENTS (Continued)

	Page
APPENDICES	74
APPENDIX A CRYSTALLIZATION.....	75
APPENDIX B AIR-SENSITIVE TECHNIQUES	87
APPENDIX C CRYSTALLOGRAPHIC INFORMATION FILE FOR 2[<i>o</i> -C ₆ H ₄ (OH) ₂]:[(CH ₂) ₆ N ₄] ADDUCT	90
APPENDIX D SUPPORTING INFORMATION FOR CHAPTER IV	98
APPENDIX E LIST OF PRESENTATIONS	99
CURRICULUM VITAE.....	100

LIST OF TABLES

Table	Page
1.1 Classification of Noncovalent Interactions with Bond Strength.....	8
1.2 Pauling Electronegativity Values, van der Waals Radii, and Ionic Radii for Selected Elements Important in Hydrogen Bonding	11
2.1 Molecular Structures of Hexamine–Phenol Adducts.....	22
3.1 Crystal Data and Structure Refinement for $2[o\text{-C}_6\text{H}_4(\text{OH})_2]:[(\text{CH}_2)_6\text{N}_4]$	36
4.1 Fractional Monoclinic Coordinates and Isotropic Atomic Displacement Parameters for $2[o\text{-C}_6\text{H}_4(\text{OH})_2]:[(\text{CH}_2)_6\text{N}_4]$	45
4.2 Anisotropic Atomic Displacement Parameters for $2[o\text{-C}_6\text{H}_4(\text{OH})_2]:[(\text{CH}_2)_6\text{N}_4]$	46
4.3 Selected Bond Distances and Angles for Hexamine in $2[o\text{-C}_6\text{H}_4(\text{OH})_2]:[(\text{CH}_2)_6\text{N}_4]$	48
4.4 Selected Bond Distances and Angles for Catechol in $2[o\text{-C}_6\text{H}_4(\text{OH})_2]:[(\text{CH}_2)_6\text{N}_4]$	49
4.5 Least Squares Plane of the Phenyl Carbon Atoms in $2[o\text{-C}_6\text{H}_4(\text{OH})_2]:[(\text{CH}_2)_6\text{N}_4]$	50
4.6 Hydrogen Bonding Geometry and Intermolecular Contacts for $2[o\text{-C}_6\text{H}_4(\text{OH})_2]:[(\text{CH}_2)_6\text{N}_4]$	51

LIST OF FIGURES

Figure	Page
1.1 Representations of Bifurcated Hydrogen-bonds	12
1.2 Schematic Drawing of Hetero- and Homo-synthons	17
2.1 Schematic Diagrams of Hexamine–Phenol Adducts	24
2.2 Structure diagram of the hexamine environment in hexamine–biphenol	27
2.3 Structure diagram of the hexamine environment in hexamine–pyrogallol	28
2.4 Structure diagram of the hexamine environment in hexamine–4-nitrocatechol–water	29
2.5 Structure diagram of the hexamine environment in hexamine–4-hydroxy-3-methoxy benzaldehyde	30
3.1 The hexamine cage-like structure for the CSD search	34
4.1 Perspective drawing of the molecular structure components of $2[o\text{-C}_6\text{H}_4(\text{OH})_2]:[(\text{CH}_2)_6\text{N}_4]$	44
4.2 Perspective drawing of two hexamine molecules and two catechol molecules	53
4.3 Packing diagram of the $2[o\text{-C}_6\text{H}_4(\text{OH})_2]:[(\text{CH}_2)_6\text{N}_4]$ adduct	55
A.1 Concentration diagram between mass fraction of crystallizing substance and temperature of the solution.	80
A.2 Methods of supersaturation creation.....	80
A.3 Schematic drawing for vapor diffusion.....	82

LIST OF FIGURES (Continued)

Figure	Page
A.4 NMR tubes and vials are often used for liquid-liquid diffusion	83
A.5 H-tube apparatus.	83
A.6 Thiele tube apparatus.	84
A.7 Sublimation apparatus.....	85
D.1 Infrared spectra of (a) catechol, (b) hexamine, and (c) catechol-hexamine...	98

LIST OF ABBREVIATIONS

\AA	Ångstrom
θ	Bragg angle or scattering angle
$^{\circ}\text{C}$	degrees celsius
β	unit cell angle
a, b, c	unit cell dimensions
e	electron
h, k, l	Miller indices
$F(000)$	total number of electrons in one unit cell of structure
R_1	crystallographic discrepancy index (unweighted)
R_2	crystallographic discrepancy index (weighted)
I	intensity
w	weight for a given reflection in the least squares refinement
$d[\]$	distance between two atoms
$U[\]$	isotropic atomic displacement parameter for the indicated atom
V	cell volume of the direct lattice
Z	number of formula units in one unit cell
$\%$	percentage
adp	atomic displacement parameter
calcd	calculated
CCDC	Cambridge Crystallographic Data Centre

LIST OF ABBREVIATIONS (Continued)

cif crystallographic information file

cm^{-1} wavenumber (per centimeter)

CSD Cambridge Structural Database

CSP crystal structure prediction

D density

DSC differential scanning calorimetry

HMT hexamethylenetetramine

FTIR Fourier transform infrared

g gram

L liter

mA milliampere

min minute

mg milligram

mL milliliter

mmol millimolar

nm nanometer

s, m, w IR strong, medium, weak

SEM scanning electron microscopy

XRD powder X-ray diffraction

CHAPTER I

INTRODUCTION

1.1 Crystallographic Background

Several thousand single crystal X-ray structures of small molecule compounds are solved every year. Crystallography has truly become a routine analytical technique for the precise determination of atomic positions, and therefore the bond lengths and bond angles of molecules within a crystal lattice. In addition to atom connectivity and stereochemistry, particularly accurate structural information about the periodic solid state is gained from the single crystal X-ray diffraction experiment, although single crystals are often very difficult to grow.

Usually, the fact that many organic substrates are solid at room temperature has little bearing on their chemistry. Due to the crystal structure is very sensitive to such parameters as temperature and pressure; the structure, and therefore the chemistry responds to variations in temperature/pressure, especially with the anisotropy of thermal expansion for continuous changes in unit cell parameters and volume, or phase transitions. An example of this in organic solids is the novel use of the structure response to external action such as decreasing temperature or increasing pressure (Boldyreva, 2003; Boldyreva, 2004) to indicate the location of hydrogen atoms when there was no direct structural information. Thus, low temperatures are used rather

often for structure determination, in order to suppress molecular motion and to improve the data quality.

Hydrogen atoms can be found very easily from neutron diffraction methods, but the relatively lower intensity of neutron sources leads to the requirement of larger crystals ($\sim 1 \text{ cm}^3$) than for X-ray diffraction methods ($\sim 10^{-3} \text{ cm}^3$). Furthermore, neutron sources are relatively rare, so neutron diffraction is rarely used when X-ray diffraction can solve a particular problem. X-ray scattering is proportional to the electron density, giving rise to the diffraction pattern, while the nuclei of the atoms do not contribute to the measured intensity.

Hydrogen is the lightest atom and contains only one electron, so the electron density measurement is sometimes difficult to detect hydrogen atom positions and to distinguish them from background. Data for determining hydrogen atom positions must be measured carefully as very accurate high quality data and proper scaling must be used. Furthermore, in X-ray diffraction, with the one exception of linear symmetric hydrogen atoms, where two X–H distances are the same, interatomic distances involving hydrogen atoms are almost always determined too short from refinement of hydrogen atoms based on X-ray diffraction data. This is due to the nature of covalent bonds where the electrons are shared between the two atoms, thus the valence electron density for covalently bonded atoms is never spherically symmetric (Müller, Herbst-Irmer, Spek, Schneider, and Sawaya, 2006) and the lack of filled core shells for hydrogen necessarily leads to shortening of the apparent X–H distance. Part of the solution to this problem is refinement of *TL* and *TLX* libration models (Rae, 1975), a routine capability in the RAELS (Rae, 2009) program suite since the 1970s, but unavailable in SHELXL and other commonly used refinement programs. A more

common part of the solution to the hydrogen atom location problem is to do crystal structure analyses based on data collected at low temperature. When the experiment is properly designed and the modeling is adequate, X-ray diffraction can be used as a tool for probing the interaction in crystals, and single crystal X-ray crystallography can also be important in obtaining reliable structural information about hydrogen atom positions.

1.2 Databases

An important consequence of the ever-growing number of crystal structure determinations has been the development of methods for the storage and retrieval of crystallographic data, and the development of several crystallographic databases. An early demonstration of the power of this new resource was the study of hydrogen bonding by structure correlation methods (Taylor and Kennard, 1984). As the number of structures in the databases has continued to increase at an accelerating pace, the use of structure correlation methods has become more widespread and they have been used to address many structure and bonding questions. Recent examples in our laboratory include the use of structure correlation to identify an erroneous structural result in the literature (Phothikanith and Haller, 2005), and to identify the previously undescribed weak $C(\delta^+) \cdots O(\delta^-)$ interaction between the carbon atom of a carbonyl group and the oxygen atom of an ether linkage (Phothikanith, 2003).

The Cambridge Structural Database, CSD (Allen, 2002), contains deposited information for organic, coordination polymer, and organometallic crystal structures determined from X-ray and neutron diffraction studies (Allen, Kennard, and Taylor, 1983) and distributed by the Cambridge Crystallographic Data Center, CCDC. The

database reached 290,000 structures in 2006 (CCDC, 2006), and currently has more than 500,000 structures (CCDC, 2009). It can be extracted (mined) using powerful search tools for studying individual bonding parameters through the polymorphism of organic and organometallic compounds, including one-dimensional, two-dimensional, and three-dimensional fragment searches, unit cell searches, and space group searches. Thus, a structure deposited at one point in time may provide valuable data on intermolecular interactions and close packing to a crystal engineer at a subsequent date. The CSD is now routinely employed as an empirical database for supramolecular synthesis, using what is known to predict what is unknown.

Crystal structure prediction can simply mean using a computer to predict the crystal structure of an organic molecule from its chemical diagram and perhaps, the crystallization conditions. The aim is the ability to predict the space group, unit cell, and atomic fractional coordinates that will be observed, should the molecule be successfully synthesized, and crystals be obtained under those conditions that allow the structure to be solved by diffraction methods. There have been four organized tests based on small organic molecules, prior to their synthesis, (Lommerse, Motherwell, Ammon, Dunitz, Gavezzotti, Hofmann, Leusen, Mooij, Price, Schweizer, Schmidt, van Eijck, Verwer, and Williams, 2000; Motherwell, Ammon, Dunitz, Dzyabchenko, Erk, Gavezzotti, Hofmann, Leusen, Lommerse, Mooij, Price, Scheraga, Schweizer, Schmidt, van Eijck, Verwer, and Williams, 2002; Day, Motherwell, Ammon, Boerrigter, Valle, Venuti, Dzyabchenko, Dunitz, Schweizer, van Eijck, Erk, Facelli, Bazterra, Ferraro, Hofmann, Leusen, Liang, Pantelides, Karamertzanis, Price, Lewis, Nowell, Torrisi, Scheraga, Arnautova, Schmidt, and Verwer, 2005; Day, Cooper, Cruz-Cabeza, Hejczyk, Ammon, Boerrigter, Tan, Valle,

Venuti, Jose, Gadre, Desiraju, Thakur, Eijck, Facelli, Bazterra, Ferraro, Hofmann, Neumann, Leusen, Kendrick, Price, Misquitta, Karamertzanis, Welch, Scheraga, Arnautova, Schmidt, Streek, Wolf, and Schweizer, 2009).

At this point in time, the results from the synthon-based approach with energy-based search, and optimization of structural features of putative structures approach are able to predict the structures of small organic molecules from only the chemical diagram and crystallization conditions in limited cases. Current CSP calculations are frequently guided by space-group statistics from the CSD and new approaches for the blind assessments continue to be tested and developed for various methods. More computer intensive methods tend to have a higher success rate, but at present time neither the computational power available nor the theory are sufficient for the reliable *ab initio* prediction of crystal structures.

1.3 Crystal Engineering

Crystal engineering is the rational design of functional molecular crystals utilizing the understanding of noncovalent interactions that govern molecular assembly to design new solid materials with desired physical and chemical properties (Desiraju. 1989). The crystal can therefore be regarded as a functional entity of a series of weak interactions with the possibility of predicting or directly anticipating the structure from the isolated molecule or molecules. Rational design of crystal structures stems from a basic understanding of the nature of the internal arrangement of atoms, molecules, and/or ions packed together that govern molecular arrangements in the lattice and provide pathways for recognition and organization to deliberate exploration of resulting materials into new crystal structure (Glusker and Trueblood,

1985). Most condensed phase systems can be considered to be supramolecular* in nature, according to Dunitz (1995), “a supermolecule par excellence”, and crystallization as an “impressive display” of supramolecular self-assembly in an ordered periodic arrangement. Since its birth, supramolecular chemistry was defined as “beyond the molecule”, bearing on the organized entities of the higher complexity that result from the association of two or more chemical species held together by intermolecular forces (Lehn 1995) to understand. Supramolecular chemistry is a “philosophy and strategy for the controlled grand assembly of complex matter”.

Supramolecular syntheses differ from molecular syntheses in that the energies involved are much smaller. This is the synthetic step, and it is not straightforward because of the emergent nature of the crystal structure. A retrosynthesis is invoked to develop a synthetic strategy that effectively simplifies the crystal structure to smaller units called synthons which are the supramolecular association via molecular fragments of the supramolecular entity. A molecule consists of functionalities or functional groups and during crystallization; these functionalities come together through a process of molecular recognition utilizing supramolecular interactions to generate supramolecular synthons (Desiraju, 2005). The main aim of crystal engineering is to the construct crystal structures from these synthons.

The engineering design of organic crystals with defined properties from this has developed with the knowledge gained from attempts to design novel materials (Gavezzotti, 1996; Aakeröy, 1997) and solid reactions (Braga and Grepioni, 2005). Another frontier area is that of functional materials as either host-guest adducts or guest-free porous solids, which may exhibit unique electronic, optical, or mechanical

* The term supramolecular comes from the combination of the Latin *supra* meaning above, with molecular, thus literally meaning above the level of the molecule.

properties (Evans, Nkansah, Hutchinson, and Rogers, 1991; Baughman and Galvão, 1993). Thus, many new organic compounds are being synthesized as materials, rather than as molecules. As a consequence, bulk properties and structure have become more important to the improved understanding of weak noncovalent contacts (Baures, Wiznycia, and Beatty, 2000) for applications, such as molecular sieves and sensors as well as other molecular level devices. One such class of compounds is organic zeolite analogues, which are one type of porous solid. An example, for which partial success in engineering crystals has been achieved, is the substituted trimesic acid compounds, which form cavity clathrates (Kolotuchin, Fenlon, Wilson, Loweth, and Zimmermann, 1995).

1.4 Supramolecular Interactions

All crystal structures of organic compounds may be formally depicted as networks with the covalently bound molecules being the nodes and the noncovalent (inter- and intra-molecular) interactions representing the stabilizing and controlling networks. Intermolecular forces were discovered by van der Waals during analysis of deviations from the ideal gas law. He noticed that molecules are sticky.

There are many ways of classifying noncovalent interactions. For the purpose of this thesis these are listed in Table 1.1 and explained below.

Table 1.1 Classification of Supramolecular Interactions with Bond Strength

Type of Interaction	Bond Energy Strength (kJ mol ⁻¹)
Ion-ion	100 – 350
Coordination	50 – 200
Dipole-dipole	5 – 80
van der Waals	< 5

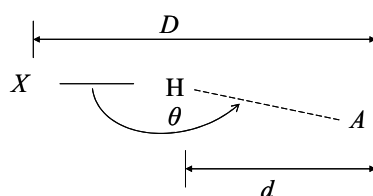
The strength of noncovalent interaction ranges are determined by weak interaction forces, like van der Waals forces, $\pi\cdots\pi$ stacking interactions, C–H $\cdots\pi$ interactions, C–H \cdots X hydrogen bond interactions (X = O, N, S), to intermediate forces such as O–H \cdots X hydrogen bonds (X = O, N), up to strong forces of charged cation-anion interactions. Intermolecular interactions in neutral organic solids are of two types: short- to medium-range isotropic or van der Waals interactions and long-range anisotropic interactions and hydrogen bonds. Dispersive force are attractive, their magnitudes are proportional to the size of molecules, and they vary as r^{-6} (r = interatomic distance). Exchange repulsion (varies as r^{-12}) balances the attractive forces to define the arrangement of molecules in the crystal based on the close-packing principle of Kitaigorodskii. Anisotropic interactions define directional preferences in the mutual recognition of molecules during crystallization. They are electrostatic in nature and operate at long range (fall off as r^{-2}). These include ionic interactions (K⁺ \cdots O), strong (O–H \cdots O) and weak hydrogen bonds (C–H \cdots O), and interactions between heteroatoms (halogen \cdots halogen). The crystal structure of a molecule is a free-energy minimum resulting from the optimization of attractive and

repulsive intermolecular interactions of varying strengths, directional preferences, and distance dependence properties.

1.5 Hydrogen Bonds

Among weak noncovalent forces, the hydrogen bond is one of the most abundant in biological systems. Hydrogen bonding is the most studied of these interactions, and it has always been well recognized that hydrogen bonding plays an important role in crystal engineering (Aakeröy, 1997), and the design and synthesis of solid-state supramolecular structures (Desiraju, 1989; Desiraju, 2001). Strong hydrogen bonds are important stabilizing factors in enzymes and are relevant to proton-transfer reactions in biological systems (Emsley, 1980; Allen, Raithby, Shields, and Taylor, 1998; Swamy, Kumaraswamy, and Kommana, 2001).

Hydrogen bonds are a particular type of dipole-dipole interaction that exists between donor sites of an electronegative atom covalently bound to a hydrogen atom ($X-H$) interacting with an acceptor atom (A) that has high electronegativity or bears a localized region or regions of electron density, such as lone pairs of electrons or π -electron density. The hydrogen bond is often represented as $X-H\cdots A$, schematically



where d is the noncovalent interaction distance from hydrogen to the acceptor atom and D is the nonbonded distance from the electronegative donor atom to the acceptor atom. As a general rule, if D is less than the sum of the van der Waals radii of X and A

and a hydrogen atom is located between X and A the interaction is considered to be a hydrogen bond.

The most stable hydrogen bonds (strongest) require both atoms X and A to have high electronegativity. The relative electronegativity of the X and A atoms affects the strength of the hydrogen bond formed. Table 1.2 lists the Pauling electronegativity values, van der Waals radii, and ionic radii for selected elements, important in hydrogen bonding. According to Pauling (1960), “the power of an atom in a molecule to attract electrons to itself”. In a molecule composed of atoms of several electronegativities the atoms with lowest electronegativity hold partial positive charges and the atoms with the highest electronegativities hold partial negative charges, hence they are dipolar or multipolar molecules.

Hydrogen atoms are more difficult to locate by X-ray crystallography than heavier atoms, making accurate geometric descriptions of hydrogen bonding based on the hydrogen positions from X-ray crystallography somewhat impractical. In this case traditional analysis has assumed that if the distance between X and A is less than the sum of their van der Waals radii, the interaction is probably a hydrogen bonding interaction. In more recent times the quality of single crystal X-ray data has been considerably improved and hydrogen atoms are now routinely located and quite often reliably refined, but the additional problem of the locus of electron density for a hydrogen atom corresponding to the bond rather than the nucleus still remains.

Table 1.2 Pauling Electronegativity Values, van der Waals Radii, and Ionic Radii for Selected Elements Important in Hydrogen Bonding.

Element	EN ^a	r_v (Å)	r_{ion} (Å)
H	2.20	1.2	
C	2.55	1.85	
N	3.04	1.54	1.71
O	3.44	1.40	1.40
S	2.58	1.85	1.84
Cl	3.16	1.80	1.81
Br	2.96	1.95	1.96
I	2.66	2.15	2.20

^a EN = Electronegativity values; r_v = van der Waals radius; r_{ion} = ionic radius.

Hydrogen bond strength (Steed and Atwood, 2000) is greatly dependent on environment. Strong hydrogen bonds are generally formed between charge donor or acceptor species, or with strong acids/bases (16–120 kJ mol⁻¹). These interactions can be nearly as strong as covalent bonds, and the charge-assisted hydrogen bonds are often sufficient to determine solid state structure and exert a marked influence on the solution and gas phase properties. In weak hydrogen bonds, such as those formed with carbon as a hydrogen-bond donor or a π -cloud acceptor, the presence of electronegative atoms near the carbon atom can significantly enhance the acidity of the proton resulting in a significantly stronger dipole, with strength rising to 2-3 times stronger than van der Waals interactions (see Table 1.1), and the range of bond strengths rising to about 12 kJ mol⁻¹. Moderate hydrogen bonds are the most studied

form and exist between neutral donors and acceptors with a general range of 16–60 kJ mol⁻¹. They commonly occur in acids, alcohols and biological molecules.

The geometry of hydrogen bond can be geometrically described by three quantities, the X to H and the H to A distances, and the X to H to A angle. Hydrogen bond angles are not necessarily linear, partly because of the tendency to form three-centered (bifurcated, see Figure 1.1) and four-centered (trifurcated) hydrogen bonds, but also because the total environment determines the interaction and the stronger covalent bonds often create constraints on the hydrogen bonds.

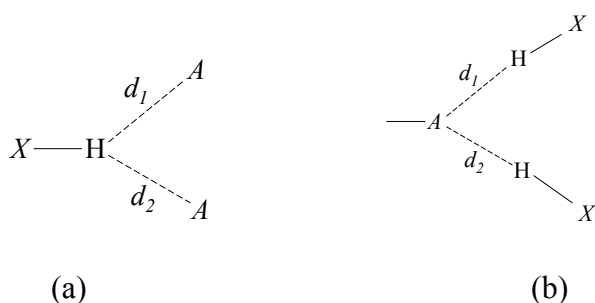


Figure 1.1 Representations of bifurcated hydrogen-bonds. (a) bifurcated donor and (b) bifurcated acceptor.

The geometrical description of hydrogen bond patterns as graph set patterns as applied by Etter to encode the complicated combination of molecules as they incorporate into crystalline materials into systematic rules was a useful advance. Bernstein and Davis systematized and extended graph set assignments and developed a set of rules to recognize, characterize, and analyze molecular crystals using graph set analysis (Bernstein, Davis, Shimoni, and Chang, 1995). The feature that makes graph set notation useful in the analysis of hydrogen bonds is the fact that even complicated networks can be reduced to combinations of simple patterns. The patterns

are specified by a designator; from infinite chains (*C*), to finite intermolecular rings (*R*), intramolecular hydrogen-bonded patterns (self, *S*), and other finite patterns (discrete, *D*). These specifications are combined with a subscript designating the number of hydrogen bond donors (*d*) and a superscript designating the number of hydrogen bond acceptors (*a*), and finally, in parentheses after the pattern designator, the total number of atoms (*n*) in the pattern, including H atoms, also called the *degree* of the pattern. This gives a total graph set descriptor, $G_d^a(n)$. Graph set analysis provided a topological method for comparing the polymorphs of iminodiacetic acid (three polymorphic structures) and considerably simplifies the understanding of hydrogen bonding similarities and differences among molecules (Etter, MacDonald, and Bernstein, 1990).

Chemists often include traditional hydrogen bond donors and acceptors into drug candidates when trying to create particular hydrogen bonding contacts (O–H \cdots O, N–H \cdots O, O–H \cdots N, or N–H \cdots N) within a macromolecular binding site. Crystal engineers in the design of new organic materials have similarly constructed supramolecular assemblies by employing strong hydrogen bonds; while also utilizing weaker intermolecular forces such as C–H \cdots O and C–H \cdots N, or the very weak halogen \cdots halogen interactions, to play a substantial role in a variety of chemical and biological phenomena. The weakest interactions are mainly stabilized by dispersive interactions or London forces in which molecules behave as oscillating dipoles transferring charge back and forth, while electrostatic contributions to the energy are relatively unimportant. The term halogen bonding is sometimes used to describe these weak interactions involving highly polarizable atoms or groups of atoms that result in short nonbonded interatomic distances observed in crystals. It is generally thought

that the halogens (Cl, Br, or I, but not F) act as acceptors, using a low-lying σ^* orbital are a potential source of supramolecular interactions.

When considering aromatic molecules, weaker $C-H\cdots\pi$ and $\pi\cdots\pi$ interactions may form due to nonuniformity of the negative charge with π -electron clouds above and below the ring plane which attract the aryl protons of the next π system, and at the same time repel π -moieties on adjacent systems. The preferred interactions include these electrostatic components, while totally eclipsed parallel face-to-face, stacked sandwich arrangement, which is correlated with dispersive interaction of fluctuating dipoles, being of lower interaction energy and less common. Solid state aryl-aryl structure is typically the herringbone motif edge-to-face $C-H\cdots\pi$ interaction, or the parallel displaced face-to-face $C-H\cdots\pi$ interaction plus dispersion interactions.

1.6 Cocrystals

The molecular packing arrangement and conformations of crystalline drug substances leading to polymorphs, hydrates, or solvates and the associated modifications of physical properties thereof have long been of interest relevant to the therapeutic value and the processing characteristics of active pharmaceutical ingredients (API) (Shenth and Grant, 2005; Almarsson, Hickey, Peterson, Morissette, Soukasene, McNulty, Tawa, MacPhee, and Remenar, 2003; Datta and Grant, 2004; Trask, Motherwell, and Jones, 2004). Organic salts give similar advantages and are relatively common and well accepted in formulations. However, there are limitations on the use of organic salts. To form an organic salt the drug is generally contains a suitable acidic or basic group that can be neutralized. Some API lack such a group,

and in other cases there are problems with the physical properties of the salts (*e.g.* their tendency to form variable solvates), which may preclude the use of salt forms.

More recently the emphasis has shifted to cocrystals to provide viable alternatives without changing the molecular structure of the API, as demonstrated by cocrystals of model APIs with improved dissolution characteristics or hydration stability (Trask, Motherwell, and Jones, 2006) while offering the same therapeutic and processing benefits. Cocrystals offer a much larger range of possibilities than the other modifications combined through the groups of compounds already approved as additives, or classified as, generally regarded as safe, by the food and drug associations (Almarsson and Zaworotko, 2004; Wenger and Bernstein, 2006; 2007; Childs, Chyall, Dunlap, Smolenskaya, Stahly, and Stahly, 2004).

For convenience, cocrystals can be defined as crystalline molecular complexes containing two or more species with essentially molecular properties that can in principle be separated into pure components with similar chemical natures to those they possess in the cocrystal.

Recent examples of cocrystal formation are quite diverse, occurring in many fields. Cocrystallization appears to be a functional tool to design materials by using defined structures or functional groups in a strong, selective, and directional way to more effectively construct new materials. Thereby, supramolecular interactions ranging from weak van der Waals interactions, to hydrogen bonds, to charge-transfer interactions, to strong coordination interactions rather than only covalent or ionic bonds are becoming extremely important in modern chemistry.

Cocrystalline materials encompass molecular compounds, molecular complexes, solvates, inclusion compounds, channel compounds, clathrates, and

possibly a few other types of multi-component crystals (Dunitz, 2003). Examples of cocrystals have existed for a long time in conductive organic crystals, nonlinear optical crystals, dyes, pigments, and agrochemicals (Etter, 1990; Fabian, Nakazumi, and Matsuoka, 1992). Cocrystal formation involving the pharmaceutical context is newer, but offers enormous potential advantages to improve physical properties of solid drug products, as illustrated by the formation of paracetamol (acetaminophen) adducts (Oswald, Allan, McGregor, Motherwell, Parsons, and Pulham, 2002), caffeine cocrystals (Bučar, Henry, Lou, Borchardt, and Zhang, 2007), and a study of quinol cocrystals with optimized hydrogen bond acceptors (Oswald, Motherwell, and Parsons, 2005). The engineering of the composition of pharmaceutical phases has truly begun (Walsh, Bradner, Fleischman, Morales, Moulton, Hornedo, and Zaworotko, 2003).

Among the weaker supramolecular interactions, hydrogen bonding is inherently one of the most robust and productive of cocrystal forms. A supramolecular synthon is a particular hydrogen bond motif (which may contain several individual hydrogen bond interactions) that can lead directly to a particular supramolecular arrangement, and thus to molecular recognition, and ultimately to self-assembly, utilizing interactions between the best hydrogen bond donors and the best hydrogen bond acceptors (Etter, 1990). In considering supramolecular synthons for a binary system, it is important to emphasize the distinction between a supramolecular homosynthon and a supramolecular heterosynthon and their implications in an appropriate circumstance for control of competitive composition, many supramolecular heterosynthons rely on the complementarities of various hydrogen bond motifs, such as carboxylic acid \cdots 2-aminopyridine, carboxylic acid \cdots urea, acid \cdots urea, acid \cdots amide, hydroxyl \cdots amine

(Shan, Bond, and Jones, 2002; Almarsson and Zaworotko, 2004; Vishweshwar, McMahon, Bis, and Zaworotko, 2006), as schematics from systematic searching of recognized cocrystals, the heterosynthon of the dimer formed by amide with carboxylic acid (a) showing in Figure 1.2, are preferring favor than either of the homosynthon of the dimer formed by carboxylic acid (b).

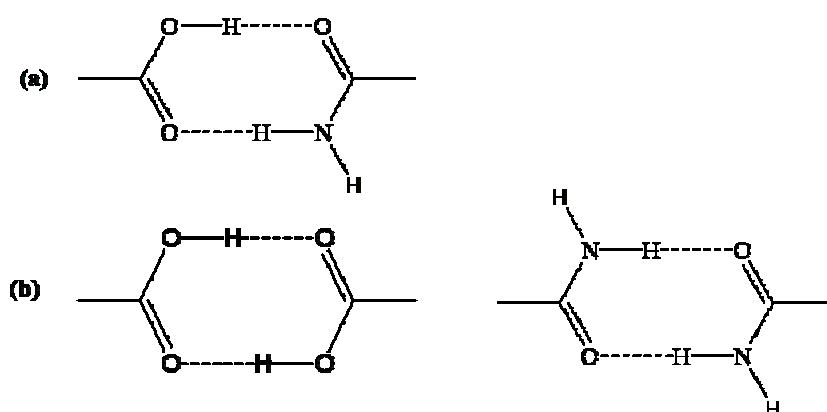


Figure 1.2 Schematic drawing of hetero- and homo-synthons. (a) heterosynthon exhibited by carboxylic acid...amide, and (b) homosynthons exhibited by carboxylic acid...carboxylic acid and amide...amide.

1.7 Practical Techniques

One of the simplest practical methods for making cocrystals is the co-grinding mechanochemical method, where two solid materials are mixed together in a mill, optionally with a small amount of solvent (solvent-drop grinding), and ground together to induce cocrystal formation. This method has proven significantly more efficient than conventional crystallization from solution for screening and preliminary synthesis of cocrystals (Trask, Motherwell, and Jones, 2004; Braga and Grepioni, 2005; Karki, Friscic, Jones, and Motherwell, 2007).

When higher purity or larger size are required (for example crystals suitable for single crystal X-ray characterization) cocrystals are most often synthesized by other crystallization processes that afford more control over relative stoichiometry and more options in separating impurities from the desired product. Crystallization provides supramolecular chemists with an opportunity to produce cocrystals as a deliberate exercise in bringing different molecular species together within one periodic crystalline lattice without making or breaking covalent bonds. Consequently, organic cocrystals are often obtained by the crystal growth method of dissolving and mixing the components and then reducing the solution volume through slow evaporation of the solvent and/or mixing solvents where the poorer solvent is less volatile so that the solubility of the solutes decrease upon evaporation in order to drive the crystallization process. The actual outcome of the crystallization is kinetically complicated by competition of all possible nuclei in the nucleation process.

Single crystal X-ray diffraction is a very powerful tool to investigate the structure of unknown compounds, and is the technique of choice for determining accurate structures of crystalline molecular inclusion complexes and molecular assemblies when suitable single crystals can be obtained. However, as computing power has increased and structure solution and refinement algorithms have become more powerful, powder X-ray diffraction for *ab initio* structure determination has come of age, and is now a common technique when suitable single crystal material is not available. Powder X-ray diffraction has traditionally been used for determining the phase purity of the bulk sample, albeit a relatively imprecise method often only able to detect components present in 5% or higher concentrations.

Vibrational spectroscopy is the classical method for the study of hydrogen bonding in condensed phases (Desiraju and Steiner, 1999). Since IR frequencies can be measured accurately, subtle effects can be detected, and its applicability ranges from the strongest to the weakest hydrogen-bond types involved in hydrogen bonding, both in solution and in the solid state. Correlations of structural and vibrational parameters have been established for various strong hydrogen-bond types. Despite its many benefits, the method is not free from drawbacks. Even for relatively simple systems on the nature of chemical bonds, spectral complexity can prevent proper interpretation.

This thesis reports the synthesis of a 2:1 catechol–hexamine adduct and improved refinement of structure based on single crystal X-ray data collected at 200 K, followed by analysis of the supramolecular structure and effects of the supramolecular interactions on the molecular structure of the component molecules in the cocrystalline material.

CHAPTER II

LITERATURE BACKGROUND

2.1 Hexamine Molecule

Hexamine, also called urotropine, methenamine, or hexamethylenetetramine, $C_6H_{12}N_4$, is the more common name in commercial uses, while methenamine is more common in its medicinal uses. It is an important agent for the chemical industry in a wide range of applications including rubber production, powdery or liquid preparation of phenolic resins, phenolic resin moulding compounds, explosives, a solid fuel tablet used for cooking while camping, and disinfectants of methenamine hippurate used to treat urinary tract infections.

The molecule is a cage-like multicyclic structure with four N atoms forming a tetrahedral arrangement and methylene groups bridging the edges of the tetrahedron. In designing solid state structures, the small symmetrical structural unit encodes four hydrogen bond motifs, introducing a unique feature to possibly facilitate rational design for molecular building of supramolecular assemblies with trigonal or tetrahedral features. The popularity of hexamine in the improved understanding of intermolecular interactions can be judged by the 440 hits of published structures in the literature found in the Cambridge Structural Database (CCDC, 2008).

The published hexamine adducts exhibit mono-, di-, tri-, and tetra-coordination via either the neutral forms of $N\cdots H-X$ ($X = N, O$) hydrogen bond interaction or the

protonated salt form of $N^+-H\cdots X^-$, charge-assisted hydrogen bond interactions, depending on the acidity of the complementary phenol or organic acid counterpart in the interaction. The four equivalent nitrogen atoms might logically be expected to favor formation of four equivalent hydrogen bonds and three-dimensional aggregation. However, one- and two-dimensional aggregation are actually much more common. The methylene protons are also anticipated to be involved in formation of $C-H\cdots O$, $C-H\cdots N$ or $C-H\cdots \pi$ weak hydrogen bonds to supplement the strong hydrogen bonds in stabilizing the supramolecular structure.

2.2 Cocrystallized Hexamine and Phenols

Interactions between amines and phenols play an important role in biological systems. Study of phenol-amine adducts has progressed over the past several decades to particular studies of hydrogen bonding and the claim that they are among the most robust and versatile synthons in crystal engineering (Fan, Vincent, and Hamilton, 1994; Desiraju, 1995). In structural engineering they are quite competitive, and phenol-amine hydrogen bonded adducts have been intensively investigated as functional tools to aid understanding of supramolecular assembly.

A subset search of the crystal structures of organic compounds cocrystallized with hexamine containing phenolic substrates (excluding inorganic atoms and macrocyclic structures) revealed thirty-one structures of neutral hexamine cocrystals and four structures of protonated hexamine adducts of phenols as listed in Table 2.1 (disordered structures are excluded from this discussion).

Table 2.1 Molecular Structures of Hexamine–Phenol Adducts.

Year	Adducts	REFCODE	Space group	R- factor (%)	Ratio
1986	Hexamine:phenylacetic acid	VIJTIR	<i>I</i> –4	7.10	1:1
1970	Hexamine:phenol	HMTTP10	<i>P</i> –3	10.10	1:3
1977	Hexamine:phenol	ZZZASG	<i>C</i> * <i>c</i> *	0.00	1:1
	Hexamine: <i>o</i> -cresol	ZZZASM	<i>Pccn</i>	0.00	1:2
	Hexamine: <i>p</i> -chlorophenol	ZZZASP	<i>P</i> 21/ <i>c</i>	0.00	1:2
	Hexamine: <i>p</i> -bromophenol	ZZZASS	<i>P</i> 21/ <i>c</i>	0.00	1:2
	Hexamine: <i>m</i> -cresol	HMTMCR	<i>Ccc</i> 2	10.90	1:2
	Hexamine:resorcinol	RSHMTA01	<i>C</i> * <i>c</i> *	0.00	1:1
	Hexamine:hydroquinone	HMTHQU	<i>P</i> 21/ <i>m</i>	9.90	1:1
1979	Hexamine:hydroquinone	HMTHQU01*	<i>P</i> 21/ <i>m</i>	5.70	1:1
	Hexamine:resorcinol	RSHMTA*	<i>C</i> 2 <i>cm</i>	11.00	1:1
1992	Hexamine: <i>p</i> -nitrophenol hydrate	BOQQAF	<i>P</i> 1	13.80	1:2
1993	Hexamine: <i>p</i> -nitrophenol	ZADFOZ	<i>P</i> –1	13.00	1:2
1997	Hexamine:4,4'-thiodiphenol	RAWCOH	<i>Pmn</i> 21	3.23	1:1
	Hexamine:4,4'-sulfonyldiphenol	RAWCUN	<i>Pmn</i> 21	4.21	1:1
	Hexamine: 4,4'-isopropylidenediphenol	RAWDAU	<i>C</i> 2/ <i>c</i>	4.01	1:1
	Hexamine:1,3,5-trihydroxybenzene	RAWDIC	<i>C</i> 2/ <i>c</i>	6.28	2:3
	Hexamine:1,1,1-tris(4-hydroxyphenyl)ethane	RAWDEY	<i>P</i> 2 ₁ 2 ₁ 2 ₁	6.36	2:1
	Hexamine:1,1,1-tris(4-hydroxyphenyl)ethane	RUNJOI	<i>Pbca</i>	6.01	1:1
1999	Hexamine:2,2'-biphenol	BOQBEO	<i>P</i> 2 ₁	6.60	1:2
2000	Hexamine:1,2,3-trihydroxybenzene	BINDIL	<i>P</i> 21/ <i>n</i>	5.40	1:1
2001	Hexamine: <i>p</i> -nitrophenol	ZADFOZ01	<i>P</i> 1	0.00	1:2
2001	Hexaminium:3,5-dinitrosalicylic acid	MILLIC	<i>P</i> 21/ <i>c</i>	5.03	1:1
	Hexamine: <i>p</i> -nitrophenol	BUQQAF01*	<i>C</i> 2	9.98	1:2
	Hexamine:2,4-dinitrophenolate monohydrate	MEVXIU	<i>P</i> –1	8.65	1:1:1
	Hexamine:2,4-dinitrophenolate monohydrate	MEVXIU01	<i>P</i> 21/ <i>m</i> 1	5.89	1:1:1

Table 2.1 (Continued)

Year	Adducts	REFCODE	Space group	R- factor (%)	Ratio
2002	Hexamine:4-nitro-catechol:water	IHERIW	<i>P-1</i>	3.98	1:2:1
	Hexamine:4-hydroxy-3-methoxy benzaldehyde	YOLQOF	<i>Pca21</i>	4.86	1:1
	Hexamine:resorcinol	RSHMTA02*	<i>Cmcm</i>	6.48	1:1
	Hexaminium:3,5-dinitrosalicylic acid	MILLIC01	<i>P21/a</i>	5.43	1:1
	Hexamine:2,4,6-trinitrophenolate	YOLQIZ	<i>P21/c</i>	5.80	3:2
2005	Hexamine:phluoroglucinol	RAWDIC01	<i>C2/c</i>	4.94	3:2
	Hexamine:methyl-3,5-dihydroxybenzoate	FEQXEF	<i>Cc</i>	2.82	1:1
	Hexamine:4-hydroxybenzoic acid	FEQXIJ	<i>P21/n</i>	4.40	1:1
2006	Hexamine:catechol	CERXIH	<i>C2/c</i>	5.10	1:2

* Disordered molecules

These adducts display two distinct behaviors:

a) The hexamine molecule utilizes multiple hydrogen bond acceptor sites to form up to four $\text{N}\cdots\text{H}-\text{O}$ hydrogen bonds depending on the availability of complementary counterparts, and

b) The polyphenols with *ortho* hydroxyl groups generally exercise the possibility of forming an $\text{O}-\text{H}\cdots\text{O}$ intramolecular hydrogen bond between the adjacent hydroxyl groups as well as strong intermolecular hydrogen bonds with both oxygen atoms, and additional weaker bonds to the phenyl ring via $\text{C}-\text{H}\cdots\text{O}$, and $\text{C}-\text{H}\cdots\pi$ hydrogen bonds and/or very weak $\pi\cdots\pi$ interactions in producing the supramolecular network (herringbone columns are especially common).

The reported adducts are illustrated in Figure 2.1, if there is more than one identical structure, only one example of that structure is presented.

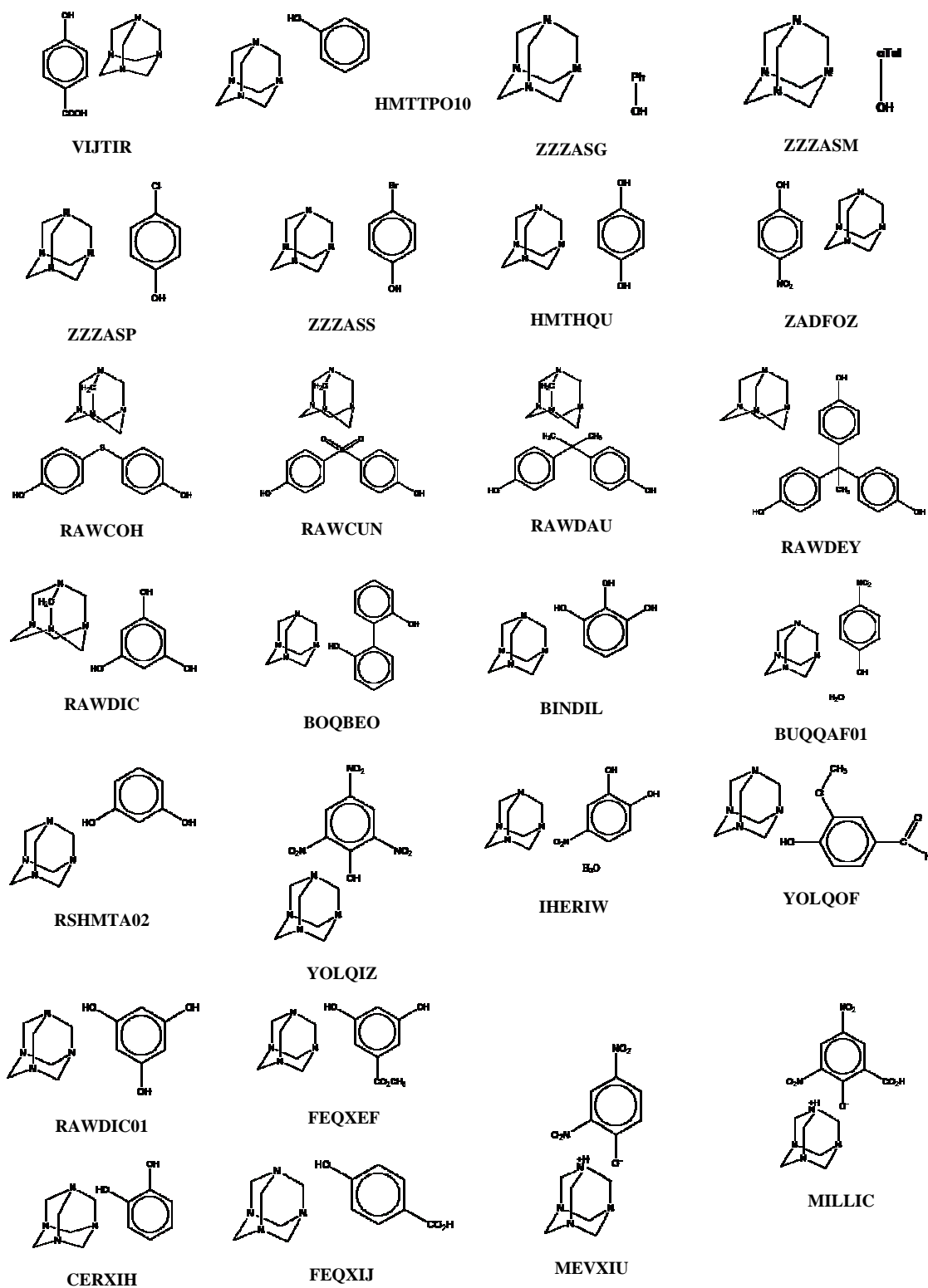


Figure 2.1 Schematic diagrams of hexamine-phenol adducts. Refcodes from CSD.

Phenol substrates can be classified into five groups based on the number of hydroxyl groups and their relative disposition on the phenyl ring: (a) mono-phenol and mono-phenol derivatives with 15 structures, (b) dihydroxybenzene and dihydroxybenzene derivatives with 7 structures, (c) bis-phenols and tris-phenols with 6 structures, (d) trihydroxybenzene with 3 structures, and (e) phenolates with 4 structures.

Seven hexamine adducts with *ortho*-substituted phenols, *i.e.* hydroxyl, phenyl, methoxy, nitro group (refcode: BOQBEO, BINDIL, MILLIC, MEVXIU, IHERIW, YOLQOF, and YOLQIZ) have been published. They use only one hydroxyl group to participate with hexamine via an O \cdots N hydrogen bond. Three of these also formed O \cdots O intramolecular hydrogen bonds providing O–C–C–O–H five-membered rings with O \cdots O distances about 2.717 (43) Å.

Mono-phenol adducts usually crystallize with hexamine to form adducts having hexamine:phenol ratios of 1:1 or 1:2, in which the hexamine acts as either a mono- or bis-acceptor of hydrogen bonds (Tse, Wong, and Mak, 1977; Mak, Yu, and Lam, 1978; Mahmoud and Wallwork, 1979), but a few examples (Jordan and Mak, 1970, Tremayne and Glidewell, 2000) have hexamine as a tris-acceptor. Similar to mono-phenol derivatives, dihydroxybenzene adducts usually crystallize with hexamine to form adducts having hexamine:phenol ratios of 1:1 and 1:2. The hydroquinone complex comprises chains of alternating hydrogen-bond donors and acceptors, in which the hexamine again acts as only a bis-acceptor. The structure of the resorcinol complex could not be solved explicitly, but it was described to be similar to that of the hydroquinone complex (Mohmoud and Wallwork, 1979; Ng, Naumov, Ibrahim, Fun,

Chantrapromma, Wojciechowski, and Hanna, 2002). In bisphenol complexes (MacLean, Glidewell, Ferguson, Gregson, and Lough, 1999) and with catechol (Daka and Wheeler, 2006) hexamine acts as a full acceptor making four O–H \cdots N hydrogen bonds.

Proton-transfer hydrogen bonding occurs in nitro substituted phenols due to the strongly electron withdrawing nature of the nitro group that increases the acidity of the hydroxyl proton. The stronger acid character results in the proton being transferred to hexamine. The protonated hexamine then acts as hydrogen bond donor to form the charge-assisted N⁺–H \cdots O[–] hydrogen bond. This phenomenon is found in the 3,5-dinitrosalicylic acid (Ng, Naumov, Drew, Wojciechowski, and Brzezinski, 2001), 2,4-dinitrophenol (Usman, Chantrapromma, and Fun, 2001), 2,4,6-trinitrophenol (Usman, Chantrapromma, Fun, Poh, and Karalai, 2002a) adducts.

Brief descriptions of selected hexamine adducts follow.

BOQBEO: Each hexamine in this adduct is an acceptor of four O–H \cdots N hydrogen bonds with four biphenols as shown in Figure 2.2. Each biphenol acts as a bridge through O–H \cdots N hydrogen bonds connecting two pairs of hexamine molecules propagating chains which interconnect to form two-dimensional sheets with $R_4^4(44)$ rings, but no O–H \cdots O hydrogen bond interactions (Maclean, Glidewell, Ferguson, Gregson, and Lough, 1999).

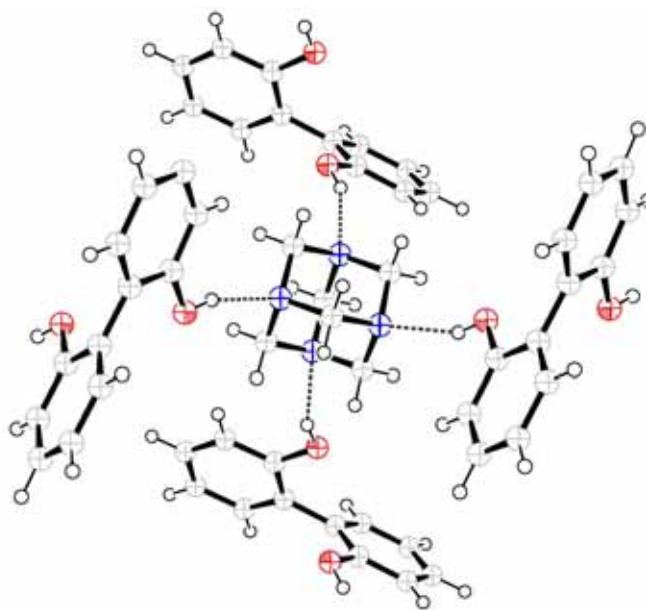


Figure 2.2 Structure diagram of the hexamine environment in hexamine-biphenol.
(BOQBEO).

BINDIL: Each hexamine in this adduct is an acceptor of three $\text{O}-\text{H}\cdots\text{N}$ hydrogen bonds from three independent hydroxyl groups of pyrogallol, as shown in Figure 2.3. Each pyrogallol forms $\text{O}-\text{H}\cdots\text{N}$ hydrogen bonds with three independent hexamine are generated two-dimensional ladder from $R_4^4(18)$ ring between two hexamine molecules and two pyrogallol molecules, there are $\text{O}-\text{H}\cdots\text{O}$ intramolecular hydrogen bond (1, 2 position) $S(5)$ motifs. Three-dimensional framework by $\text{C}-\text{H}\cdots\pi$ interaction and the pyrogallol column like herringbone column (Tremayne and Glidewell, 2000).

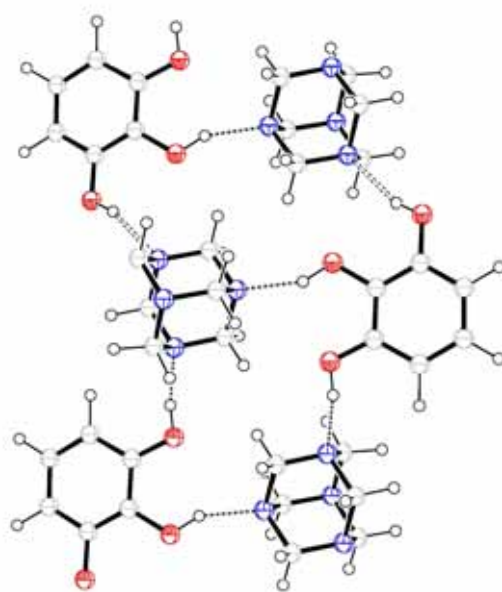


Figure 2.3 Structure diagram of the hexamine environment in hexamine–pyrogallol.

(BINDIL).

IHERIW: With a 1:2:1 ratio of hexamine–4-nitrocatechol–water, the hexamine acts as an acceptor site of $\text{O}-\text{H}\cdots\text{N}$ hydrogen bonds with two N atoms, as shown in Figure 2.4. One molecular layer contains six different hydrogen-bonded ring patterns, namely those linking: the hexamine molecule with two symmetry-independent 4-nitrocatechol molecules with $\text{O}-\text{H}\cdots\text{N}$ and weak $\text{C}-\text{H}\cdots\text{O}$ hydrogen bonds, $R_3^3(14)$; two hexamine molecules to two 4-nitrocatechol molecules via $\text{O}-\text{H}\cdots\text{N}$ hydrogen bonds, $R_4^4(18)$; four symmetry-related 4-nitrocatechol molecules to two symmetry-related hexamine molecules, $R_6^6(26)$; two symmetry independent 4-nitrocatechol molecules produce a six-membered ring conformation via intermolecular $\text{C}-\text{H}\cdots\text{O}$ and $\text{O}-\text{H}\cdots\text{O}$ motifs, $R_2^2(6)$; a water molecule to a nitrocatechol molecule via $\text{O}-\text{H}\cdots\text{O}$ and $\text{C}-\text{H}\cdots\text{O}$ hydrogen bonds to provide another

six-membered motif, $R_2^1(6)$; and finally two symmetry-related water molecules to two symmetry-related 4-nitrocatechol molecules in an $R_4^4(28)$ motif.

Another interesting feature of this structure is the two symmetry-independent 4-nitrocatechol molecules which demonstrate the two limiting conformations of the hydroxyl groups. In one form of 4-nitrocatechol one hydroxyl hydrogen atom forms a strong intramolecular O–H \cdots O (O \cdots O = 2.725 Å) hydrogen bond motif, $S(5)$, giving the *syn* conformation, while the other 4-nitrocatechol has the two hydroxyl groups in the *anti* conformation, stabilized by multiple hydrogen-bond interactions to its neighbors. (Chantrapromma, Usman, Fun, Poh, and Karalai, 2002),

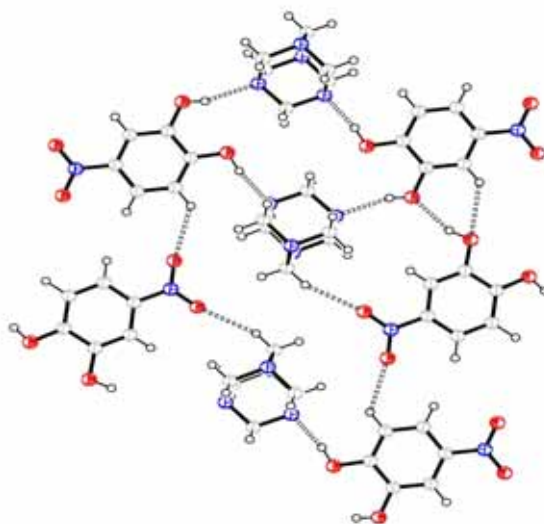


Figure 2.4 Structure diagram of the hexamine environment in hexamine–4-nitrocatechol–water. (IHERIW).

YOLQIZ: Each hexamine in this adduct is an acceptor of only one O–H \cdots N hydrogen bonds from 4-hydroxy-3-methoxybenzaldehyde, as shown in Figure 2.5. There are two intermolecular C–H \cdots O interactions which link hexamine into molecular sheets further stabilized by C–H \cdots π interactions. The hydroxyl hydrogen

atom forms the strong intramolecular O–H···O hydrogen bond to the *ortho* methoxy group in the five membered-ring pattern, $S(5)$, exhibiting a bifurcated donor similar to that found in the catechol structure (Usman, Chantrapromma Fun, Poh and Karalai, 2002b).

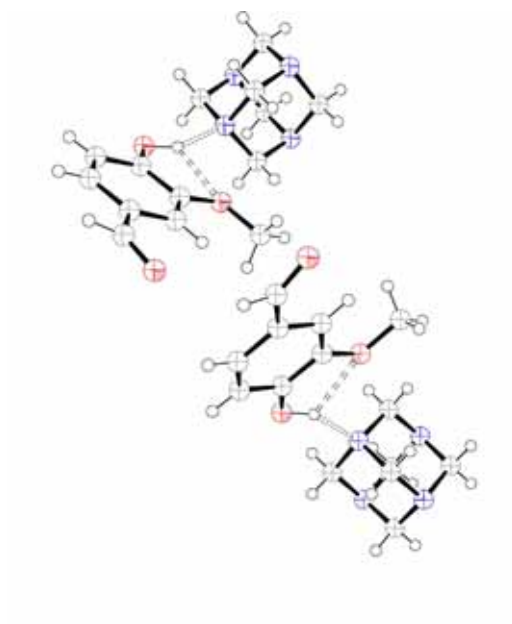


Figure 2.5 Structure diagram of the hexamine environment in hexamine-4-hydroxy-3-methoxy benzaldehyde. (YOLQIZ).

CHAPTER III

EXPERIMENTAL

3.1 Materials

3.1.1 Chemical Reagents

All chemical reagents were used as received without further purification. All chemicals except solvents were characterized prior to use by powder X-ray diffraction (XRD) and infrared spectroscopy.

Catechol (1,2-dihydroxybenzene or pyrocatechol, $C_6H_4(OH)_2$) was obtained in HPLC grade (assay $\geq 98.5\%$) from Sigma-Aldrich Chemie GmbH.

Hexamine (1,3,5,7-tetraazatricyclo[3.3.1.1^{3,7}]decane or hexamethylene-tetramine, $C_6H_{12}N_4$) was obtained in HPLC grade (98.5% assay) from Asia Pacific Specialty Chemicals Ltd. Company.

Solvents were used as received without further purification. Only small amounts of materials were prepared.

- a) Acetone, $(CH_3)_2CO$, RPE-ACS grade, Carlo Erba Reagent
- b) Acetonitrile, CH_3CN , AR (ACS) grade, Mallinkrodt Chemicals
- c) Benzene, C_6H_6 , ACS grade, Carlo Erba Reagent
- d) Chloroform, $CHCl_3$, AR analytical product, Mallinkrodt Chemicals
- e) Dichloromethane, CH_2Cl_2 , BDH
- f) Diethyl ether, $(CH_3CH_2)_2O$, Carlo Erba Reagent

- g) Dimethyl sulfoxide (DMSO), $(\text{CH}_3)_2\text{SO}$, Sigma-Aldrich
- h) Ethyl alcohol, $\text{CH}_3\text{CH}_2\text{OH}$, Carlo Erba Reagent
- i) Isopropyl alcohol, $(\text{C}_3\text{H}_8\text{O})$, BDH
- j) Methyl alcohol, CH_3OH , Carlo Erba Reagent
- k) Toluene, $\text{C}_6\text{H}_5\text{CH}_3$, ChromAR grade, Mallinkrodt Chemicals

3.1.2 Laboratory Materials

- a) Filter paper, Whatman diameter 47 mm, standard grades
- b) Hypodermic syringe, 10 mL made from borosilicate hard glass, Mira
- c) Parafilm
- d) Schlenk flasks
- e) Weighing paper
- f) Thermometer
- g) Nitrogen, H.P. grade 99.95%, TIG company

3.2 Equipment

3.2.1 Laboratory Equipment

- a) Desiccator
- b) Analytical balance
- c) Hot plate stirrer
- d) Melting point apparatus
- e) Optical microscope
- f) Laboratory oven

3.2.2 Instrumentation

Single Crystal X-ray Diffraction

X-ray intensity data for a selected specimen were collected on a Bruker-Nonius Kappa CCD diffractometer, equipped with graphite monochromated Mo $K\alpha$ radiation ($\lambda = 0.71073 \text{ \AA}$), 0.5 mm *ifg* capillary collimator, and an Oxford Cryostream apparatus (Oxford Cryosystems, 1997).

Powder X-ray Diffraction (XRD)

Powder X-ray diffraction patterns were obtained using a Siemens-Bruker D5005 powder X-ray diffractometer equipped with a Ni-filtered Cu $K\alpha$ radiation source and operated at 35 kV/35 mA. All XRD data were collected under the same experimental conditions, in the angular range $3^\circ \leq 2\theta \leq 50^\circ$ and scan speed of $0.5/0.02^\circ \theta$ angle. Typically, the data was expressed as a plot between intensity of diffraction peaks and 2θ angle. The positions of diffraction peaks were compared with patterns in the PDF database for identification of compounds.

Infrared Spectroscopy (IR)

Infrared spectra were obtained using a Perkin-Elmer Spectrum GX FTIR spectrophotometer, to take the mid IR spectra of samples ($4000\text{--}400 \text{ cm}^{-1}$). The solid sample and KBr pellet were dried at 110°C for at least 1 hour before mixing KBr with sample in a mortar and pestle. The ground powder was pressed into a transparent disk using a hydraulic press with an equivalent weight of about 10 tons for 1 minute. The spectra were collected as 13 summed scans to give a resolution of 4 cm^{-1} .

3.2.3 Databases

Cambridge Structural Database Search

The Cambridge Structural Database (CSD; Version 5.29 with updates on January 2008) was searched to analyze the frequency of hexamine molecules in deposited structures. The cage-like structure of hexamine (Figure 3.1) was utilized to

search and provided 440 total hits. Of these, the neutral form of hexamine molecule acting as hydrogen bond acceptor with O–H donor components (phenols and organic acids) accounted for 54 hits, with phenols accounting for 31 hits. The protonated hexamine as a hydrogen bond donor with O[–] acceptors accounted for 24 hits, of which 4 were phenolates.

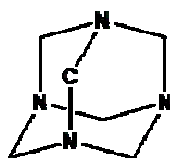


Figure 3.1 The hexamine cage-like structure for the CSD search.

Thirty-five published adducts of hexamine are formed with mono-, di-, or triphenols and phenol derivatives. These and their CSD Refcodes are listed in Table 2.1 along with the stoichiometric ratios of their components.

3.3 Procedures

3.3.1 Crystallization of Hexamine and Catechol

Various factors were adjusted for optimization and glassware was oven-dried at 100 °C for 2 hours before use. Stoichiometric quantities of the two components were adjusted by varying molar ratios of hexamine and catechol at 1:1 and 1:2. Pure solvents or mixed solvents used to dissolve the components include methanol, water, chloroform, diethyl ether, dichloromethane, acetone/methanol, water/methanol, water/acetone, and dichloromethane/water.

The solutions were allowed to crystallize by conventional crystal growth as slow evaporation, vapor diffusion, and liquid-liquid diffusion.

Hexamine (0.3505 g, 2.5 mmol) was dissolved in chloroform (5 mL) by warming to reflux temperature, catechol (0.5506 g, 5.0 mmol) was dissolved in diethyl ether (5 mL) maintained under a nitrogen atmosphere until a clear solution was obtained, and the two solutions mixed together. All solution operations were carried out under a nitrogen atmosphere using Schlenk techniques.

3.3.2 Structure Solution and Refinement

The structure was solved by direct methods (SIR97) and refined by full matrix least-squares refinement based on F^2 using the SHELX97 software package. *ORTEP-III* and Diamond 2.1 were used for graphics illustrations.

Structure Refinement

In the final cycles, all nonhydrogen atoms were refined anisotropically, hydrogen atom coordinates were refined without restraints, and atomic displacement parameters for the hydrogen atoms were refined with the constraint of equivalence for the two hydroxide hydrogen atoms, the four phenyl hydrogen atoms, and the six independent methylene hydrogen atoms. The crystal data and structure refinement for cocrystal of hexamine–catechol are given in Table 3.1.

Table 3.1 Crystal Data and Structure Refinement for 2[*o*-C₆H₄(OH)₂]:[(CH₂)₆N₄].

Empirical formula	C ₁₈ H ₂₄ N ₄ O ₄
Stoichiometry	2:1
Formula weight	360.41
Temperature	200 (2) K
Wavelength	0.71073 Å
Crystal system	Monoclinic
Space group	<i>C2/c</i>
Unit cell dimensions	$a = 23.5925 (7) \text{ Å}$ $b = 6.8339 (2) \text{ Å}$ $c = 13.1856 (3) \text{ Å}$ $\beta = 123.1362 (17)^\circ$
Volume	1780.17 (8) Å ³
<i>Z</i>	4
Density (calculated)	1.345 Mg m ⁻³
Absorption coefficient	0.097 mm ⁻¹
<i>F</i> (000)	768
Crystal size	0.35 x 0.37 x 0.48 mm ³
θ range for data collection	5.12 – 28.73°
Limiting indices	$0 \leq h \leq 31, 0 \leq k \leq 9, -17 \leq l \leq 14$
Reflections collected/unique	2260/1952
Completeness to θ	97.9 % to 28.73°
Data/restraints/parameters	2260/0/173
Goodness-of-fit on F^2	1.174
Final <i>R</i> indices [$I > 2\sigma(I)$]	$R_I = 0.0457, wR_2 = 0.1003$
<i>R</i> indices (all data)	$R_I = 0.0605, wR_2 = 0.1155$
Largest diff peak and hole	0.20 (4) and -0.25 e Å ⁻³

CHAPTER IV

SUPRAMOLECULAR STRUCTURE OF

COCRYSTALLINE CATECHOL AND HEXAMINE

4.1 Introduction

The crystal structure of the highly symmetric hexamethylenetetramine or urotropine, $(\text{CH}_2)_6\text{N}_4$, (hexamine) molecule was determined at room temperature in 1923 (Dickenson and Raymond, 1923). Adducts of hexamine with organic molecules, including phenols, have subsequently been widely investigated (Ng, Naumov, Drew, Wojuciechowski, and Brzezinski, 2002; Pinheiro, Gardon, and Chapuis, 2003). Phenol-amine adducts are widely used for the study of hydrogen bonding, partly because combinations of phenols and amines play an important role in biological systems due to the ability of the two components to link by strong $\text{O}-\text{H}\cdots\text{O}$, $\text{O}-\text{H}\cdots\text{N}$, or $\text{N}-\text{H}\cdots\text{O}$ intermolecular hydrogen bonds, and also because these adducts are among the most robust and versatile supramolecular synthons in crystal engineering (Fan, Vincent, Geib, and Hamilton, 1994).

Hydrogen bonding is one of the most significant noncovalent interactions occurring in many kinds of materials and in structural chemistry and biology. It can exist in biological and pharmaceutical systems and can display highly directional nature and relative strength to provide a variety of possible architectures. In nature, hydrogen bonds are often found at the microscopic scale in molecular aggregates and

at the macroscopic scale in crystals, and play a crucial role in biological phenomena. Observation of this role has been part of the rationale for the development of new solid state materials through crystal engineering (Lehn, 1995; Desiraju, 1989).

Strong hydrogen bonds play a particularly important structure-directing role. Many recent publications on molecular recognition are concerned primarily with strong $\text{N-H}\cdots\text{X}$ and $\text{O-H}\cdots\text{X}$ ($\text{X} = \text{O}, \text{N}$) hydrogen bonds for their wide implications in biological systems, such as in enzymes where strong hydrogen bonds are an important stabilizing factor and are relevant to proton-transfer reactions.

Other recent progress has focused on exploring hydrogen bonding involving hydrogen attached to carbon, rather than the highly electronegative atoms. $\text{C-H}\cdots\text{O}$, $\text{C-H}\cdots\text{N}$, and $\text{C-H}\cdots\pi$ hydrogen bonds are involved in the formation of supramolecular assemblies and in determining their properties, as in heme systems where they have been identified as a key feature in the excitonic coupling in malaria pigment related heme aggregates (Puntharod, Webster, Bambery, Asghari-Khiavi, Safinejad, Rivadeh, Langford, Haller, and Wood, 2010). Their use, especially when acting in concert, is increasing rapidly in the design of new materials by crystal engineering.

Etter and coworkers applied mathematical graph set analysis to hydrogen bond patterns, and introduced the idea of systematic rules (Etter, 1990; Etter, MacDonald, and Bernstein, 1990) to the hydrogen bond combination of molecules as they incorporate into crystalline materials. Etter's graph set ideas were systematized and extended, and the rules to recognize, characterize, and analyze molecular crystals using graph set analysis were further developed (Bernstein, Davis, Shimoni, and Chang, 1995). The feature that makes graph set notation useful in the analysis of

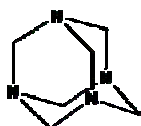
hydrogen bonds is the fact that even complicated networks can be reduced to combinations of simple patterns. The patterns are specified by a designator; from infinite chains (*C*), to finite intermolecular rings (*R*), intramolecular hydrogen-bonded patterns (self, *S*), and other finite patterns (discrete, *D*). These specifications are combined with a subscript designating the number of hydrogen bond donors (*d*) and a superscript designating the number of hydrogen bond acceptors (*a*), and finally, in parentheses after the pattern designator, the total number of atoms (*n*) in the pattern, including H atoms, also called the *degree* of the pattern. This gives a total graph set descriptor, $G_d^a(n)$.

Design of materials is of course not restricted to pure molecular compounds. An increasingly important group of new materials is cocrystals, and within this group of multicomponent molecular complexes are the crystalline structures that involve active pharmaceutical ingredients (APIs) in an alternative form to the traditionally accepted crystalline forms of polymorphs, solvates/hydrates, and salts. The search for new cocrystals has augmented the findings of motif or synthon chemistry (Steiner, 2002) and led to many families of crystalline molecular solids classified according to chemical reactivity, electrical, optical, magnetic, or other properties; or by applications such as conductive organic crystals, nonlinear optical crystals, dyes and pigments, and agrochemicals. Many of these involve molecular components with particular structural motifs for achieving desired physical properties in the resulting material.

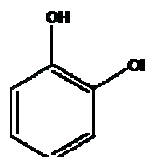
The Cambridge Structure Database, CSD, through structure correlation (Burgi and Dunitz, 1992), has been important for discovering and understanding the interactions of various individual structural motifs (Allen, 2002). However,

understanding of the crystal packing has generally been a result of knowing the structure, and the elusive goal of predicting crystal structures has been difficult to achieve, even for pure compounds (Day, Cooper, Cruz-Cabeza, Hejczyk, Ammon, Boerrigter, Tan, Valle, Venuti, Jose, Gadre, Desiraju, Thakur, Eijck, Facelli, Bazterra, Ferraro, Hofmann, Neumann, Leusen, Kendrick, Price, Misquitta, Karamertzanis, Welch, Scheraga, Arnautova, Schmidt, Streek, Wolf, and Schweizer, 2009). When designing materials using noncovalent supramolecular linkages it is important to use appropriate molecules, meeting the requirements of compatible geometric interactions as well as energetic interactions, which will lead to the ultimate goal of controlled formation of chains or of two- or three-dimensional ribbons, sheets, spheres, helices, tubes, and so on. In the event of alternative supramolecular arrangements, those having proportionately more strong hydrogen bonds are more likely to be realized.

The current study examines the phenol-amine cocrystalline adduct of:



1,3,5,7-tetraazatricyclo[3.3.1.1.3,7]decane, or hexamine



1,2-dihydroxybenzene, or catechol

In general amines are both good hydrogen bond acceptors and donors at their nitrogen atoms. The amine chosen here is a tertiary amine so does not have N–H donors, only the nitrogen lone-pair acceptors. However, six CH₂ groups are each bound to two nitrogen atoms, increasing their acidity and strengthening their weak hydrogen bond donor properties. The catechol molecule has two hydroxyl groups, each with two lone-pairs on oxygen and one O–H motif, thus both strong hydrogen bond acceptors

and donors. In addition the four phenyl ring C–H groups are weak donors and the delocalized π -electron clouds are weak hydrogen bond acceptors.

Search of the version 5.29 CSD database (CCDC, 2008) revealed 77 hits of hexamine molecules crystallized as organic cocrystalline compounds or molecular salts. Neutral hexamine molecular complexes account for 53 of the reported structures, and protonated hexamine molecular salts account for the remaining 24 structures. The 298 K structure of hexamine–catechol has been communicated (Daka and Wheeler, 2006). Herein, we report the structural determination at 200 K and present detailed supramolecular analysis, including graph set analysis of hydrogen bond patterns.

4.2 Materials and Methods

Preparation of Hexamine–catechol Adduct

All chemicals were used as received without further purification. Hexamine–catechol adduct was formed when 0.35 g (2.5 mmol) of hexamine in 5 mL of warm chloroform were added to 0.55 g (5.0 mmol) of catechol in 5 mL of diethyl ether and then allowed to evaporate slowly over a few days, giving transparent colorless crystalline product. FTIR (ν_{max}/cm^{-1}): 3441 m, 3428 m, 3125 m, 3072 m, 3050 m, 3028 m, 2967 m, 2887 m, 2760 m, 2734 m, 2716 m, 2663 m, 2589 m, 2465 w, 1600 – 2000 w, 1661 m, 1588 m, 1518 m, 1466 s, 1392 m, 1383 m, 1368 m, 1274 s, 1267 s, 1241 s, 1230 s, 1100 m, 1051 w, 1011 s, 928 w, 915 w, 856 w, 818 m, 802 m, 759 w, 741 s, 689 s, 669 w, 561 w, 512 w.

X-ray Crystallographic Study

A transparent, colorless chunk of $2[o\text{-C}_6\text{H}_4(\text{OH})_2]:[(\text{CH}_2)_6\text{N}_4]$ cut from a larger block-shaped crystal was mounted on a hollow glass fiber using cyanoacrylate glue. The monoclinic $C2/c$ space group contains eight catechol and four hexamine molecules ($Z = 4$), that is, one catechol molecule and one-half a hexamine molecule in the asymmetric unit. Data collection was performed on a Kappa CCD diffractometer equipped with graphite monochromated Mo $K\alpha$ radiation ($\lambda = 0.71073 \text{ \AA}$), 0.5 mm *ifg* capillary collimator, and an Oxford Cryosystems low temperature device operating at 200 K. All twenty nonhydrogen atoms were located by direct methods using *SIR97* (Altomare, Burla, Camalli, Cascarano, Giacovazzo, Guagliardi, Moliterni, Polidori, and Spagna, 1999) and refined by full matrix least-squares refinement based on F^2 using the *SHELXL97* software (Sheldrick, 1997). Crystal data and a summary of refinement parameters are given in Table 3.1.

All nonhydrogen atoms were refined anisotropically and all hydrogen atoms were easily located from a Fourier electron density difference map and included in the refinement, initially with restraints; the CH hydrogen atoms in catechol were restrained with a common bond length and a common isotropic atomic displacement parameter, *adp*, as were the OH hydrogen atoms in catechol and the CH hydrogen atoms in hexamine (6 of 48 possible coordinate and U_{iso} variables for the twelve hydrogen atoms). When the preliminary refinement converged, the restraints and constraints on the hydrogen atoms were removed.

First, the distance restraint on the hydroxyl hydrogen atoms was removed (5 added variables) and $d[\text{O1-H1}]$ contracted while $d[\text{O2-H2}]$ expanded. Second, the *adp* constraint on the hydroxyl hydrogen atoms was removed (1 added variable) and $U[\text{H1}]$ expanded while $U[\text{H2}]$ contracted. Third, the $d[\text{C-H}]$ restraints were removed

(28 added variables) and the distances observed to remain near their restrained values. Finally, the *adp* constraints on hydrogen atoms attached to carbon atoms were removed (8 added variables) and the *U* values observed to remain at realistic values. Thus, the final cycles refined all nonhydrogen atoms as anisotropically vibrating contributions and all hydrogen atoms as isotropically vibrating contributions in unconstrained least-squares refinement. The molecular components of hexamine–catechol adduct are shown, with the labeling scheme for the crystallographically unique atoms indicated thereon, as an *ORTEP-III* (Burnett and Johnson, 1996; Farrugia, 1997) perspective drawing in Figure 4.1. Fractional monoclinic coordinates and isotropic atomic displacement parameters (Table 4.1) and anisotropic atomic displacement parameters (Table 4.2) follow. A standard crystallographic information file (*cif* file) is included as Table C.1 in Appendix C.

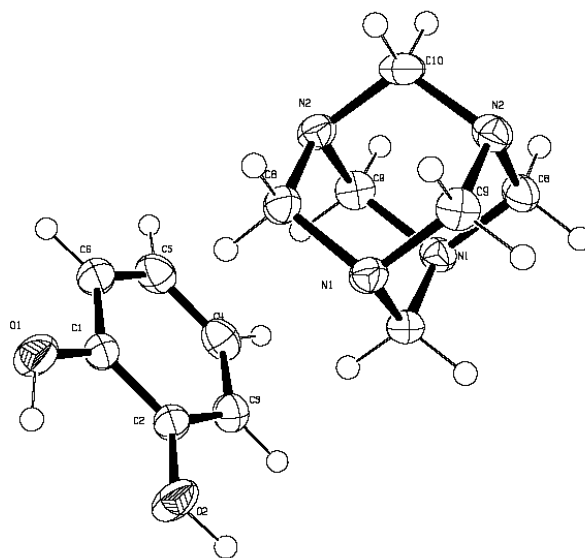


Figure 4.1 Perspective drawing of the molecular structure components of $2[o\text{-C}_6\text{H}_4(\text{OH})_2]:[(\text{CH}_2)_6\text{N}_4]$. The atom-labeling scheme is indicated on

the drawing. Atomic displacement parameters are represented as ellipsoids drawn at the 50% probability level.

Table 4.1 Fractional Monoclinic Coordinates and Isotropic Atomic DisplacementParameters (\AA^2) for $2[o\text{-C}_6\text{H}_4(\text{OH})_2]:[(\text{CH}_2)_6\text{N}_4]$.

Atom ^a	<i>x</i>	<i>y</i>	<i>z</i>	U_{eq} ^b or U_{iso}
C1	0.6508 (1)	0.0441 (2)	0.6543 (1)	0.028 (1)
C2	0.6379 (1)	−.1068 (2)	0.7103 (1)	0.027 (1)
C3	0.6748 (1)	−.1193 (2)	0.8356 (1)	0.031 (1)
C4	0.7258 (1)	0.0150 (2)	0.9058 (1)	0.035 (1)
C5	0.7393 (1)	0.1627 (2)	0.8506 (1)	0.037 (1)
C6	0.7017 (1)	0.1785 (2)	0.7251 (1)	0.035 (1)
O1	0.6145 (1)	0.0639 (2)	0.5312 (1)	0.040 (1)
O2	0.5879 (1)	−.2353 (2)	0.6358 (1)	0.040 (1)
C7	$\frac{1}{2}$	0.1138 (3)	$\frac{3}{4}$	0.027 (1)
C8	0.5041 (1)	0.3598 (2)	0.6260 (1)	0.028 (1)
C9	0.5857 (1)	0.3594 (2)	0.8404 (1)	0.028 (1)
C10	$\frac{1}{2}$	0.6063 (3)	$\frac{3}{4}$	0.029 (1)
N1	0.4585 (1)	0.2337 (2)	0.6406 (1)	0.025 (1)
N2	0.5461 (1)	0.4858 (2)	0.7329 (1)	0.027 (1)
H1	0.5877 (1)	−.047 (4)	0.478 (2)	0.078 (2)
H2	0.5828 (1)	−.337 (3)	0.682 (2)	0.071 (7)
H3	0.6644 (8)	−.227 (3)	0.8728 (15)	0.038 (4)
H4	0.7514 (10)	0.005 (3)	0.9950 (18)	0.047 (5)
H5	0.7760 (10)	0.258 (3)	0.8996 (18)	0.052 (5)
H6	0.7095 (9)	0.283 (3)	0.6826 (16)	0.046 (5)
H7	0.4692 (7)	0.029 (2)	0.7623 (13)	0.025 (4)
H8A	0.5348 (8)	0.274 (2)	0.6147 (15)	0.034 (4)
H8B	0.4759 (8)	0.442 (2)	0.5525 (14)	0.030 (4)
H9A	0.6127 (8)	0.440 (2)	0.9154 (15)	0.034 (4)
H9B	0.6171 (8)	0.276 (3)	0.8290 (15)	0.036 (4)
H10	0.4731 (8)	0.691 (3)	0.6762 (14)	0.035 (4)

^a The numbers in parentheses are the estimated standard deviations in the least significant digits.^b Equivalent isotropic displacement parameters, U_{eq} are given for all atoms refined anisotropically.

Table 4.2 Anisotropic Atomic Displacement Parameters (\AA^2) for
 $2[o\text{-C}_6\text{H}_4(\text{OH})_2]:[(\text{CH}_2)_6\text{N}_4]$.

Atom ^a	U_{11}	U_{22}	U_{33}	U_{23}	U_{13}	U_{12}
C1	0.032 (1)	0.028 (1)	0.028 (1)	−.0037 (5)	0.0192 (6)	−.0040 (5)
C2	0.027 (1)	0.028 (1)	0.029 (1)	−.0039 (5)	0.0158 (5)	−.0048 (5)
C3	0.032 (1)	0.033 (1)	0.029 (1)	−.0005 (5)	0.0170 (6)	−.0002 (6)
C4	0.030 (1)	0.041 (1)	0.029 (1)	−.0072 (6)	0.0134 (6)	0.0001 (1)
C5	0.032 (1)	0.039 (1)	0.039 (1)	−.0147 (6)	0.0190 (6)	−.0101 (6)
C6	0.040 (1)	0.032 (1)	0.041 (1)	−.0083 (6)	0.0269 (7)	−.0113 (6)
O1	0.055 (1)	0.036 (1)	0.028 (1)	−.0033 (4)	0.0217 (5)	−.0168 (8)
O2	0.045 (1)	0.040 (1)	0.027 (1)	−.0031 (4)	0.0152 (5)	−.0217 (5)
C7	0.034 (1)	0.020 (1)	0.031 (1)	0	0.0204 (8)	0
C8	0.035 (1)	0.026 (1)	0.025 (1)	−.0027 (5)	0.0185 (6)	−.0055 (5)
C9	0.025 (1)	0.030 (1)	0.027 (1)	0.0005 (5)	0.0116 (5)	0.002 (5)
C10	0.037 (1)	0.018 (1)	0.029 (1)	0	0.0158 (8)	0
N1	0.030 (1)	0.022 (1)	0.025 (1)	−.0024(4)	0.0154 (4)	−.0045 (4)
N2	0.030 (1)	0.024 (1)	0.026 (1)	−.0012(4)	0.0153 (5)	−.0050 (4)

^a The numbers in parentheses are the estimated standard deviations in the least significant digits.

4.3 Results and Discussion

Molecular Structure

The asymmetric unit of structure contains one half of one molecule of hexamine, located on a 2-fold axis through atoms C7 and C10, and one molecule of catechol, giving the hexamine:catechol stoichiometric ratio of 1:2. The refined hydrogen atom distances^{*} for aromatic –CH, –OH, and methylene –CH are in the ranges 0.984 (19) – 0.993 (21) Å, 0.952 (27) – 0.977 (24) Å, and 0.998 (17) – 1.010(17) Å, respectively, with mean values 1.004 (6)Å, 0.964 (18)Å, and 0.988 (4)Å, respectively.

The interatomic bond distances and angles of hexamine (Table 4.3) have normal values (Allen, Kennard, Watson, Brammer, Orpen, and Taylor, 1987) as approximately pyramidal structure about 1.468 (14) Å as reported in structure correlation (Burgi and Dunitz, 1992). The geometric parameters for the hexamine molecule are comparable with those of uncomplexed hexamine obtained from neutron diffraction at 120 K (Kampermann, Ruble, and Craven, 1994), and with those in other hexamine adducts. The mean N–C and/or the average values of the ranges of the N–C bond lengths, and of the C–N–C and N–C–N bond angles in the hexamine moiety are 1.4747 (16) Å, 109.73 (10)° and 112.02 (12)°, respectively.

*

Estimated standard derivations on individual structure parameters are derived from the least-squares refinement process and those on mean values are calculated from the individual parameter variances from the mean value assuming they are all in the same population.

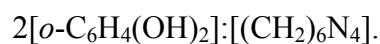
Table 4.3 Selected Bond Distances and Angles (Å, °) for Hexamine in
 $2[o\text{-C}_6\text{H}_4(\text{OH})_2]:[(\text{CH}_2)_6\text{N}_4]$.

Atoms ^{a, b}	Distances	Atoms	Angles
C7 ⁽ⁱ⁾ –N1	1.4725 (14)	C7–N1–C8	108.19 (9)
C8–N1	1.4707 (16)	C8–N1–C9 ⁽ⁱ⁾	108.44 (10)
C8–N2	1.4781 (16)	C7–N1–C9 ⁽ⁱ⁾	108.16 (9)
C9–N1 ⁽ⁱ⁾	1.4740 (17)	C8–N2–C9	108.52 (10)
C9–N2	1.4772 (16)	C8–N2–C10	107.75 (9)
C10–N2	1.4758 (15)	C9–N2–C10	108.19 (9)
		N1 ⁽ⁱ⁾ –C7–N1	112.34 (14)
		N1–C8–N2	111.93 (10)
		N1 ⁽ⁱ⁾ –C9–N2	111.62 (10)
		N2–C10–N2 ⁽ⁱ⁾	112.19 (14)

^a The numbers in parentheses are the estimated standard deviations in the least significant digits.

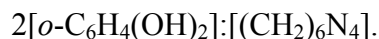
^b Symmetry code: (i) $-x+1, y, -z+3/2$.

Interatomic bond distances and angles of the catechol molecule are listed in Table 4.4. The mean sum of angles about catechol C atoms is 359.99 (1)°, the sum of the six C–C–C angles is 719.98°, and the mean of the two C–O distances is two 1.365 (1) Å, which is the same as the average (1.362 Å) found among phenols by structure correlation (Allen, Kennard, Watson, Brammer, Orpen, and Taylor, 1987). The absolute planarity of the aromatic ring can also be seen in the insignificant displacements of the carbon atoms from the mean plane through the six phenyl carbon atoms (Table 4.5).

Table 4.4 Selected Bond Distances and Angles (Å, °) for Catechol in

Atoms ^a	Distances	Atoms	Angles
C1–O1	1.3661 (16)	C6–C1–C2	119.42 (13)
C2–O2	1.3641 (16)	O1–C1–C6	118.91 (12)
C1–C2	1.3959 (19)	O1–C1–C2	121.66 (12)
C2–C3	1.3862 (18)	C1–C2–C3	119.93 (12)
C3–C4	1.389 (2)	O2–C2–C1	116.61 (12)
C4–C5	1.379 (2)	O2–C2–C3	123.46 (12)
C5–C6	1.390 (2)	C2–C3–C4	120.33 (13)
C6–C1	1.3890 (19)	C2–C3–H3	118.25 (11)
C3–H3	0.987 (18)	C4–C3–H3	121.41 (10)
C4–H4	0.988 (19)	C3–C4–C5	119.80 (13)
C5–H5	0.993 (21)	C3–C4–H4	119.33 (12)
C6–H6	0.984 (19)	C5–C4–H4	120.85 (12)
		C4–C5–C6	120.28 (13)
		C4–C5–H5	120.65 (12)
		C6–C5–H5	119.07 (11)
		C5–C6–C1	120.22 (14)
		C5–C6–H6	122.59 (11)
		C1–C6–H6	117.19 (11)
		C1–O1–H1	115.21 (14)
		C2–O2–H2	111.08 (13)

^a The numbers in parentheses are the estimated standard deviations in the least significant digits.

Table 4.5 Least Squares Plane of the Phenyl Carbon Atoms in

Equation: $19.121(8)x - 3.998(3)y - 6.158(7)z = 8.242(6)$

Atom ^{a, b}	Displacement (Å)	Atom	Displacement (Å)
*C1	−0.0032 (10)	H1	+0.184 (25)
*C2	+0.0084 (10)	H2	+0.048 (22)
*C3	−0.0066 (10)	H3	−0.005 (17)
*C4	−0.0005 (10)	H4	−0.021 (20)
*C5	+0.0057 (11)	H5	+0.024 (19)
*C6	−0.0038 (10)	H6	−0.009 (18)
O1	−0.0184 (21)		
O2	+0.0251 (20)		

^a The numbers in parentheses are the estimated standard deviations in the least significant digits.

^b Atoms included in the least squares plane calculation are indicated by an asterisk.

Strong Intra- and Inter-molecular Hydrogen Bonds

As result of hydrogen bonding geometry and interaction of 1:2 hexamine and catechol adduct in Table 4.6, a strong intramolecular O–H \cdots O hydrogen bond interaction is presented, in each catechol moiety, *S*(5) hydrogen bond pattern, (O1–H1 \cdots O2 (O \cdots O = 2.724 (1) Å, 103.0 (16)°), similar to previously reported adducts with α -dihydroxyl phenols, including in 1,2,3-trihydroxybenzene (O \cdots O = 2.732 – 2.772 Å, Tremayne and Glidewell, 2000), 4-nitrocatechol (O \cdots O = 2.725 Å, Chantrapromma, Usman, Fun, Poh, and Karalai, 2002) and 4-hydroxy-3-methoxybenzaldehyde (O \cdots O = 2.703 Å, Usman, Chantrapromma, Fun, Poh, and Karalai, 2002).

O1–H1 also participates in a second hydrogen bond, to the N1 atom of hexamine creating strong O–H \cdots N hydrogen bond, (O1 \cdots N1 = 2.822 (1) Å, 160 (2)°) as part of $R_2^2(8)$ pattern (included weak C8–H8b \cdots O2 hydrogen bonding) thus O1–H1 is a bifurcated strong hydrogen bonds.

Table 4.6. Hydrogen Bonding Geometry and Intermolecular Contacts (Å, °) for $2[o\text{-C}_6\text{H}_4(\text{OH})_2]:[(\text{CH}_2)_6\text{N}_4]$.

$D\text{--H}\cdots A$ ^{a, b, c}	$D\text{--H}$	$\text{H}\cdots A$	$D\cdots A$	$D\text{--H}\cdots A$
Strong hydrogen bonds				
O1–H1 \cdots N1 ⁽ⁱ⁾	0.95 (3)	1.91 (3)	2.822 (1)	160 (2)
O2–H2 \cdots N2 ⁽ⁱⁱ⁾	0.98 (2)	1.81 (2)	2.760 (1)	162 (2)
O1–H1 \cdots O2	0.95 (3)	2.35 (2)	2.724 (1)	103.0 (16)
Weak hydrogen bond				
C8–H8b \cdots O2 ⁽ⁱ⁾	0.995 (16)	2.518 (15)	3.026 (2)	111.4 (11)
C9–H9b \cdots C _g ⁽ⁱ⁾	1.010 (17)	2.638		
C6–H6 \cdots C _g ⁽ⁱⁱⁱ⁾	0.984 (19)	2.74		

^a The numbers in parentheses are the estimated standard deviations in the least significant digits.

^b Symmetry codes: (i) $-x+1, -y, -z+1$; (ii) $x, y-1, z$; (iii) $-x+3/2, y-1/2, -z+3/2$.

^c C_g is the aromatic centroid ring C1 – C6.

O2–H2 participates in one strong O2–H2···N2 hydrogen bond ($O2\cdots N2 = 2.760$ (1) Å, 162 (2)°) and one weak C8–H8b···O2 hydrogen bond ($C8\cdots O2 = 3.026$ (1) Å, 111.4 (11)°).

The O1–H1···N1 hydrogen bond is shorter due to the intramolecular O1–H1···O2 interaction making H1 a bifurcated hydrogen-bond donor and resulting in weaker donor strength to N1, while O2–H2 donates to only one strong hydrogen bond, thus retaining its strong donor ability. Furthermore, O2 act as a bifurcated acceptor using both lone pairs to form hydrogen bonds, increasing the acidity of H2 and thus the donor strength of O2–H2.

The four-membered neighbor molecules, as shown in Figure 4.2, lie on *bc* plane create one element of the 1-D hydrogen-bonded chain which is composed of two catechols and two hexamines. The interconnection between these members are linked by intermolecular O1–H1···N1 hydrogen bond, and then linked to the second crystallographically independent N atom in a second hexamine molecule *via* O2–H1···N2 hydrogen bonds. One element of the resulting 1-D chain contains four different hydrogen-bonded ring patterns, namely those linking the intramolecular hydrogen bond of catechol molecule [*S*(5)], the single catechol molecule to a single hexamine molecule, $R_2^2(8)$, and two symmetry-related catechol molecules to two symmetry-related hexamine molecules as first-level graph set which only one strong (O1···N1) hydrogen bond and involved one weak (C8···O2), $R_4^4(10)$ designation, and a second-level which included two catechol and two hexamine which only strong (O1···N1 and O2···N2) hydrogen bond, $R_4^4(18)$ designation.

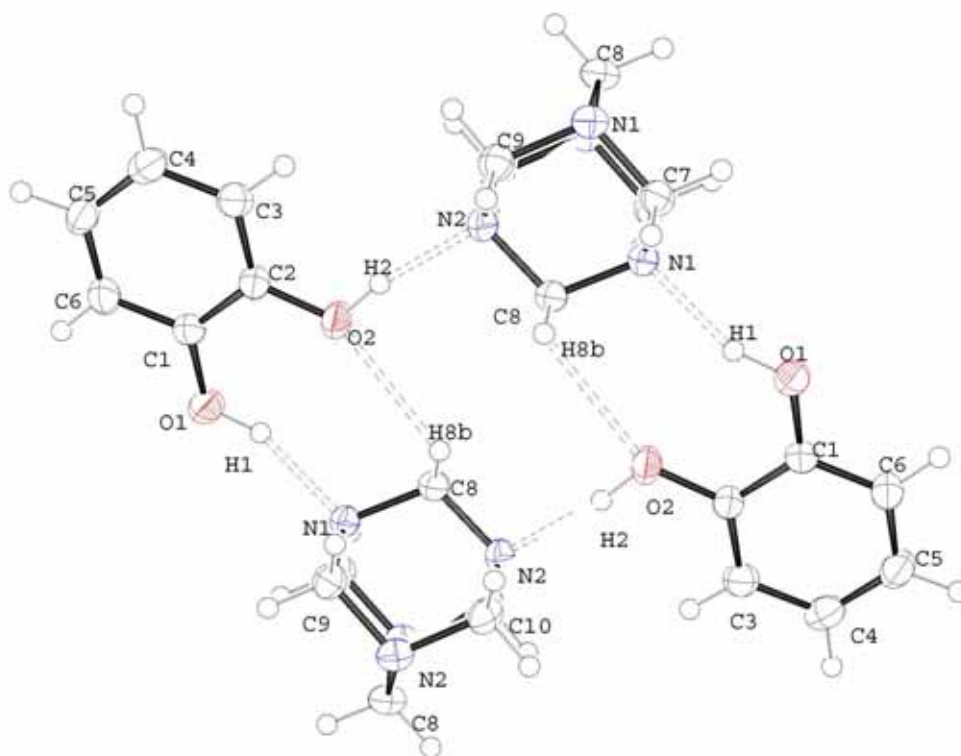


Figure 4.2 Perspective drawing of two hexamine molecules and two catechol molecules. The dashed lines denote the strong O–H \cdots O and O–H \cdots N hydrogen-bond interactions. Atomic displacement parameters are represented as ellipsoids drawn at the 50% probability level.

Thus, all four nitrogen atoms in the hexamine molecules act as hydrogen bond acceptors with the –OH groups of four independent catechol molecules. This differs from the majority of previously reported phenol–catechol systems, in which hexamine acts as only a double acceptor of hydrogen bonds, and rather less frequently as an acceptor of only one hydrogen bond (Usman, Chantrapromma, Fun, Poh, and Karalai, 2002), three hydrogen bonds (Tremayne and Glidewell, 2000), or as in this case, the full complement of four hydrogen bonds (Maclean, Glidewell, Ferguson, Gregson and Lough, 1999).

In addition to the weak C–H \cdots O interaction described in the previous section, there are several C–H \cdots π interactions. The phenyl rings pack into columns with adjacent phenyl rings interacting by C6–H6 \cdots π edge-to-face hydrogen bonds propagated by the 2_1 -screw axis, the catechol chains are arranged in the herringbone-like pattern. The columns are additionally linked by the strong O2–H2 \cdots N2 and the weak C9–H9b \cdots π interactions to hexamine as shown in Figure 4.3.

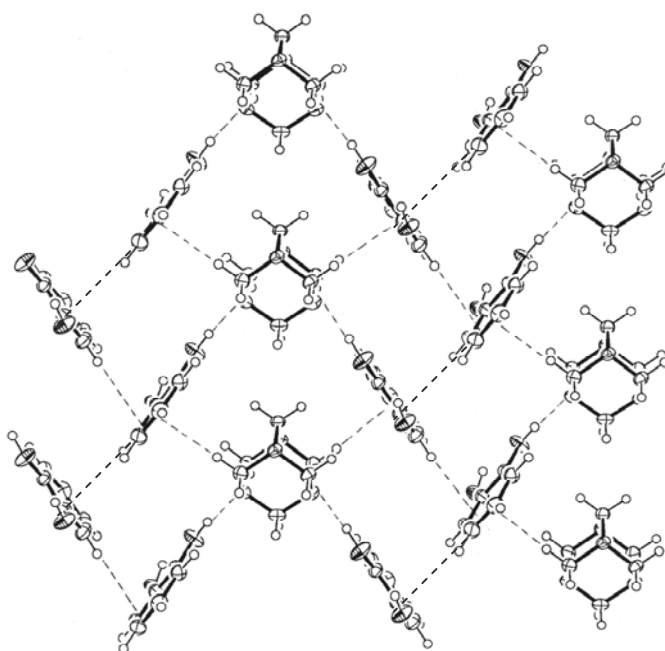


Figure 4.3 Layer packing diagram of the $2[o\text{-C}_6\text{H}_4(\text{OH})_2]:[(\text{CH}_2)_6\text{N}_4]$ adduct. Shows the formation [010] sheet that links catechol herringbone chain with hexamine.

Effect of Supramolecular Structure on Molecular Structure

There are several intriguing suggestions of trends in the structure parameters found herein. It was noted in the experimental description that on removing the equal distance and equal *adp* restraints on the hydroxyl hydrogen atoms that the O1–H1 distance contracted and U_{H1} expanded, both consistent with stronger hydrogen bonding interaction on O2–H2. A more conventional measure of relative hydrogen bond strength comes in the form of the O–H \cdots N interactions. The O2–H2 \cdots N2 interaction is significantly shorter (stronger) at 2.7608 (15) Å compared to the O1–H1 \cdots N1 interaction at 2.8227 (15) Å (41 σ shorter). The interaction angles are the same, $\sim 161^\circ$. The stronger hydrogen bonding interaction also manifests itself in the hexamine molecule where the C–N distances fall into two groups. The shorter distances, average 1.4724 (16) Å, are to N1 while the longer distances, average = 1.4770 (12) Å, are to N2. While the average values are within 2 σ , the bimodal distribution of the bond lengths, consistently correlated with the other parameters noted indicates the difference is significant.

Infrared Spectroscopy

Vibrational spectra of hexamine–catechol adduct, broad, medium-intense bands located in the $3600\text{--}3340\text{ cm}^{-1}$ region in the IR spectra correspond to manifestation of stretching vibration of O–H groups participating in O–H \cdots N and O–H \cdots O strong

hydrogen bonds. The bands of aromatic C–H stretching of sp^2 C–H of benzene ring also occur as bands in the ranges of $3134\text{--}2600\text{ cm}^{-1}$, the bands of relevant out-of-plane (oop) bending modes were observed in the IR spectra in the $900\text{--}690\text{ cm}^{-1}$ region. Many weak combination and overtone bands appear between $2000\text{--}1667\text{ cm}^{-1}$ region, these weak absorptions and the vibration markers for the pattern as *ortho*-substitution of phenyl ring is one strong band at 741 cm^{-1} . Strong, IR active bands observed in the spectra in the $1260\text{--}1000\text{ cm}^{-1}$ region are characteristic for C–O stretching agrees with conjugation of the oxygen with the ring concerning the O–H \cdots O and O–H \cdots N hydrogen bond.

A pair of strong broad bands at 1392 and 1383 cm^{-1} , and aromatic C–C ring stretch absorptions often occur in range at $1660\text{--}1600\text{ cm}^{-1}$ and also with 1475 cm^{-1} . In addition to this band, an O–H in-plane bending absorption is usually found near 1360 cm^{-1} for the neat samples of phenols. In the latter band usually overlaps the C–H bending vibration for the methyl group at 1375 cm^{-1} . C–N stretch occurs in the range $1350\text{--}1000\text{ cm}^{-1}$ as a medium to strong band, amines absorb from $1250\text{--}1000\text{ cm}^{-1}$. The methylene ($\text{--CH}_2\text{--}$) groups give rise to two C–H stretching bands at 2962 cm^{-1} (asym) and 2887 cm^{-1} (sym). The asymmetric mode generates a longer dipole moment and greater intensity than the symmetric mode. The C–H bending vibration band occurring at 1466 cm^{-1} is generally present for CH_2 scissoring of the methylene group.

4.4 Conclusions

The presence of both strong O–H \cdots O intramolecular hydrogen-bonding and O–H \cdots N intermolecular hydrogen-bonding interactions between two hydroxyl groups

and tertiary nitrogen atoms were produced by cocrystallization of hexamine and catechol. The hexamine–catechol adduct is essentially ensured by strong O–H \cdots N and weak C–H \cdots O and C–H $\cdots\pi$ hydrogen bonding connecting hexamine and catechol are present into a two-dimensional network. The network stacks using additional weak intermolecular interactions to give a three-dimensional supramolecular network.

CHAPTER V

SUMMARY AND CONCLUSION

Understanding of molecular assembly utilizing supramolecular interactions is one of the most recent attempts to rational design and the development of new solid materials. Self-organization of the complementary components of supramolecular entities allows application of the knowledge information of molecular recognition phenomena to control or determine resulting properties. Cocrystals are solid materials that incorporate multiple components in a common lattice and thereby can create new structural-property relationships for the new materials. Such materials are of great current interest in pharmaceutical processes and materials science.

Control of the crystallization process and conditions is important to provide crystals of suitable size and purity for the single crystal X-ray diffraction experiment; perhaps all the more so for cocrystal formation. An additional factor in this regard is control of the synthons involved. Selection of motifs that form strong associations in solution will enhance the probability that they persist into the lattice, assuring successful cocrystallization. Other factors affecting crystallization include solvent, nucleation and growth, mechanics, time, and perhaps even factorial design experiments with closely related sets of conditions.

In this thesis, hexamine, a highly symmetric molecule with four tertiary amine strong hydrogen bond acceptor sites, and catechol, with two strong hydrogen bond

donor sites were utilized. A CSD search for adducts of the hexamine cage molecule with organic acids or alcohols with at least one O–H \cdots N or N⁺–H \cdots O[–] interaction produced 77 hits. Phenols account for 54 hits. Surprisingly, only three examples occur wherein all four potential O \cdots N interactions are realized. In addition to the strong O \cdots N interactions, these systems usually illustrate herringbone structure from the phenyl ring systems, further stabilizing the cocrystals, or perhaps by acting in concert successfully competing with the stronger O \cdots N interactions.

The described hydrogen bond motif with the strong N-atom hydrogen bond acceptors of hexamine all participate in hydrogen bonds with the strong O–H donors of catechol. One hydroxyl group participates in both intramolecular ($d[\text{O}\cdots\text{O}] = 2.724$ (1) Å, 103.0 (16)°) hydrogen bonding motifs with graph theory designation $S(5)$, and intermolecular ($d[\text{O}\cdots\text{N}] = 2.822$ (1) Å, 160 (2)°) strong hydrogen bonds making this hydroxyl site a bifurcated hydrogen bond donor. The other hydroxyl group participates in one strong hydrogen bond donor interaction ($d[\text{O}\cdots\text{N}] = 2.760$ (1) Å, 162 (2)°), one strong hydrogen bond acceptor interaction (from O1–H1 above), and one weak hydrogen bond acceptor interaction ($d[\text{C}\cdots\text{O}] = 3.026$ (1) Å, 111.4 (11)°) with symmetry-related hexamine molecules. One hexamine molecule links four catechol molecules; two via intermolecular O–H \cdots N and C–H \cdots O hydrogen bonds in a ring conformation motif, graph set designation $R_2^2(8)$, which link through the hexamine molecules to form one dimensional chains of alternating catechol and hexamine molecules. Two symmetry-related catechol molecules link to symmetry-related (half) hexamine molecules to two symmetry-related catechol molecules via (the other half-hexamine molecules) two strong intermolecular O–H \cdots N hydrogen bonds forming local graph set designation, $R_4^4(18)$ and if the weak C–H \cdots O hydrogen

bond is included instead of one O–H \cdots N, graph set designation $R_4^4(10)$. The phenyl ring π -clouds of the catechol molecule pack together via intermolecular C–H $\cdots\pi$ edge-to-face hydrogen bonds propagated by 2_1 -screw axes to generate herringbone columns linked together by which are reinforced and to form sheets by hexamine molecules via weak C–H $\cdots\pi$ hydrogen bonds.

Future Studies

The environments of the two hydroxyl groups are different suggesting there should be two OH stretching bands in the IR. The region has broad bands and is difficult to interpret. Thus substituting deuterium on the hydroxyl group may clarify the OH stretching region.

The hydrogen bonding in the cocrystal is dominated by the O–H \cdots N hydrogen bonds, but other important components also exist. Replacing one or both hydroxyl groups with similar sized groups or similar donor/acceptor groups offers an opportunity to observe the interplay of these interactions.

REFERENCES

REFERENCES

- Aakeröy, C. B. (1997). Crystal Engineering: Strategies and Architectures. **Acta Crystallogr., Sect. B: Struct. Sci.** 53: 569–586.
- Aakeröy, C. B. and Salmon, D. J. (2005). Building Co-crystals with Molecular Sense and Supramolecular Sensibility. **CrystEngComm** 7(72): 439–448.
- Allen, F. H. (2002). The Cambridge Structural Database: A Quarter of a Million Crystal Structures and Rising. **Acta Crystallogr., Sect. B: Struct. Sci.** 58: 380–388.
- Allen, F. H., Kennard, O., and Taylor, R. (1983). Systematic Analysis of Structural Data as a Research Technique in Organic Chemistry. **Acc. Chem. Res.** 16: 146–153.
- Allen, F. H., Kennard, O., Watson, D. G., Brammer, L., Orpen, A. G. and Taylor, R. (1987). Tables of Bond Lengths Determined by X-ray and Neutron Diffraction. Part 1. Bond Lengths in Organic Compounds. **J. Chem. Soc. Perkin Trans. 2**: S1–S19.
- Allen, F. H. and Motherwell, S. W. D. (2002). Applications of the Cambridge Structural Database in Organic Chemistry and Crystal Chemistry. **Acta Crystallogr., Sect. B: Struct. Sci.** 58: 407–422.
- Allen, F. H., Raithby, P. R., Shields, G. P. and Taylor, R. (1998). Probabilities of Formation of Bimolecular Cyclic Hydrogen-Bonded Motifs in Organic Crystal Structures: A Systematic Database Analysis. **Chem. Commun.** 1043–1044.

- Almarsson, Ö., Hickey, M. B., Peterson, M. L., Morissette, S. L., Soukasene, S., McNulty, C., Tawa, M., MacPhee, J. M. and Remenar, J. F. (2003). High-Throughput Surveys of Crystal Form Diversity of Highly Polymorphic Pharmaceutical Compounds. **Cryst. Growth Des.** 3(6): 927–933.
- Almarsson, Ö. and Zaworotko, M. J. (2004). Crystal Engineering of the Composition of Pharmaceutical Phases. Do Pharmaceutical Co-crystals Represent a New Path to Improved Medicines? **Chem. Commun.** 1889–1896.
- Altomare, A., Burla, M. C., Camalli, M., Cascarano, G. L., Giacovazzo, C., Guagliardi, A., Moliterni, A. G. G., Polidori, G. and Spagna, R. (1999). SIR97: A New Tool for Crystal Structure Determination and Refinement. **J. Appl. Cryst.** 32: 115–119.
- Atwood, J. L., Davies, J. E. D. and MacNicol D. D., eds (1984). Inclusion Compounds: Physical Properties and Applications. Academic Press, London.
- Baughman, R. H. and Galvão, D. S. (1993). **Nature** 365: 365.
- Baures, P. W., Wiznycia, A. and Beatty, A. M. (2000). Hydrogen Bonding Isosteres: Bimolecular Carboxylic Acid and Amine-*N*-oxide Interaction Mediated via CH \cdots O Hydrogen Bonds. **Bioorg. Med. Chem.** 8: 1599–1605.
- Bernstein, J., Davis, R. E., Shimon, L. and Chang, N.-L. (1995). Patterns in Hydrogen Bonding: Functionality and Graph Set Analysis in Crystals. **Angew. Chem., Int. Ed. Engl.** 34: 1555–1573.
- Boldyreva, E. V. (2003). High-Pressure Studies of the Anisotropy of Structural Distortion of Molecular Crystals. **J. Mol. Struct.** 647: 159–179.
- Boldyreva, E. V. (2004). High-Pressure Studies of the Hydrogen Bond Networks in Molecular Crystals. **J. Mol. Struct.** 700: 151–155.

- Braga, D. and Grepioni, F. (2005). Making Crystals from Crystals: A Green Route to Crystal Engineering and Polymorphism. **Chem. Commun.** 3635–3645.
- Bučar, D.-K., Henry, R. F., Lou, X., Borchardt, T. B. and Zhang, G. G. Z. (2007). A Hidden Co-crystal of Caffeine and Adipic Acid. **Chem. Commun.** 525–527.
- Burgi, H.-B. and Dunitz, J. D. (1992). Structure Correlation. VCH, Weinheim.
- Burnett, M. N. and Johnson, C. K. (1996). ORTEP-III: Oak Ridge Thermal Ellipsoid Plot Program for Crystal Structure Illustrations. Report ORNL-6895, Oak Ridge National Laboratory, Oak Ridge Tennessee.
- CCDC, (2006). Cambridge Structure Database, Version 5.27 with August 2006 updates, Cambridge Crystallographic Data Centre, Cambridge, UK.
- CCDC, (2008). Cambridge Structure Database, Version 5.29 with January 2008 updates, Cambridge Crystallographic Data Centre, Cambridge, UK.
- Chantrapromma, S., Usman, A., Fun, H.-K., Poh, B.-L. and Karalai, C. (2002). Hexamethylenetetramine–4-nitrocatechol–water (1/2/1). **Acta Crystallogr., Sect. C: Cryst. Struct. Commun.** 58: o675–o677.
- Childs, S. L., Chyall, L. J., Dunlap, J. T., Smolenskaya, V. N., Stahly B. C. and Stahly, G. P. (2004). Crystal Engineering Approach to Forming Cocrystals of Amine Hydrochlorides with Organic Acids. Molecular Complexes of Fluoxetine Hydrochloride with Benzoic, Succinic and Fumaric Acids. **J. Am. Chem. Soc.** 126: 13335–13342.
- Coupar, P. I., Glidewell, C. and Ferguson, G. (1997). Crystal Engineering Using Bisphenol and Trisphenols. Complexes with Hexamethylenetetramine (HMTA): Strings, Multiple Helices and Chains-of-Rings in the Crystal Structures of the Adducts of HMTA with 4,4'-Thiodiphenol (1/1), 4,4'-Sulfonyldiphenol (1/1),

4,4'-Isopropylidenediphenol (1/1), 1,1,1-Tris(4-hydroxyphenyl)ethane (1/2) and 1,3,5-Trihydroxybenzene (2/3). **Acta Crystallogr., Sect. B: Struct. Sci.** 53: 521–533.

Daka, P. and Wheeler, K. A. (2006). Bis(1,2-dihydroxybenzene) Hexamethylenetetramine. **Acta Crystallogr., Sect. E: Struct. Rep. Online** 62(12): o5477–o5479.

Datta, S. and Grant, D. J. W. (2004). Crystal Structures of Drugs: Advances in Determination, Prediction and Engineering. **Nat. Rev. Drug Discovery.** 3: 42–57.

Day, G. M., Motherwell, W. E. S., Ammon, H. L., Boerrigter, S. X. M., Valle, R. G. D., Venuti, E., Dzyabchenko, A., Dunitz, J. D., Schweizer, B., van Eijck, B. P., Erk, P., Facelli, J. C., Bazterra, V. E., Ferraro, M. B., Hofmann, D. W. M., Leusen, F. J. J., Liang, C., Pantelides, C. C., Karamertzanis, P. G., Price, T. C., Lewis, T. C., Nowell, H., Torrisi, A., Scheraga, H. A., Arnautova, Y. A., Schmidt, M. U. and Verwer, P. (2005). A Third Blind Test of Crystal Structure Prediction. **Acta Crystallogr., Sect. B: Struct. Sci.** 61(5): 511–527.

Day, G. M., Cooper, T. G., Cruz-Cabeza, A. J., Hejczyk, K. E., Ammon, H. L., Boerrigter, S. X. M., Tan, J. S., Valle, R. G. D., Venuti, E., Jose, J., Gadre, S. R., Desiraju, G. R., Thakur, T. S., van Eijck, B. P., Facelli, J. C., Bazterra, V. E., Ferraro, M. B., Hofmann, D. W. M., Neumann, M. A., Leusen, F. J. J., Kendrick, J., Price, S. L., Misquitta, A. J., Karamertzanis, P. G., Welch, G. W. A., Scheraga, H. A., Arnautova, Y. A., Schmidt, M. U., Streek, J. V. D., Wolf, A. K. and Schweizer, B. (2009). Significant Progress in Predicting the Crystal Structures of Small Organic Molecules – A Report on the Fourth Blind Test. **Acta Crystallogr., Sect. B: Struct. Sci.** 65(2): 107–125.

- Desiraju, G. R. (1989). *Crystal Engineering: The Design of Organic Solids*. Elsevier, Amsterdam.
- Desiraju, G. R. (1995). Supramolecular Synthons in Crystal Engineering – A New Organic Synthesis. **Angew. Chem., Int. Ed. Engl.** 34: 2311–2327.
- Desiraju, G. R. (2001). Crystal Engineering: Outlook and Prospects. **Curr. Sci.** 81(8): 1038–1042.
- Desiraju, G. R. (2003). Crystal and Co-crystal. **CrystEngComm** 5(82): 466–467.
- Desiraju, G. R. (2005). Chemistry–The Middle Kingdom. **Curr. Sci.** 8: 374–380.
- Desiraju, G. R. and Steiner, T. (1999). *The Weak Hydrogen Bond in Structural Chemistry and Biology*. Oxford University Press, Oxford. 253–266.
- Dey, A. and Desiraju, G. R. (2006). Dimorphs of 4'-Amino-4-hydroxy-2'-methylbiphenyl: Assessment of Likelihood of Polymorphism in Flexible Molecules. **CrystEngComm** 8: 477–481.
- Dey, A., Kirchner, M. T., Vangala, V. R., Desiraju, G. R., Mondal, R. and Howard, J. A. K. (2005). Crystal Structure Prediction of Aminols: Advantages of a Supramolecular Synthon Approach with Experimental Structures. **J. Am. Chem. Soc.** 127: 10545–10559.
- Dickinson, R. G. and Raymond, A. L. (1923). The Crystal Structure of Hexamethylene-tetramine. **J. Am. Chem. Soc.** 45(1): 22–29.
- Dunitz J. D. and Desiraju, G. R. (eds) (1995). *Perspectives in Supramolecular Chemistry: The Crystal as a Supramolecular Entity*. Wiley, Amsterdam.
- Dunitz J. D. (2003) Crystal and Co-crystal: a Second Opinion. **CrystEngComm** 5(91): 506–506.
- Emsley, J. (1980). Very Strong Hydrogen Bonding. **Chem. Soc. Rev.** 9: 91–124.

- Etter, M. C. (1990). Encoding and Decoding Hydrogen-Bond Patterns of Organic Compounds. **Acc. Chem. Res.** 23(4): 120–126.
- Etter, M. C., MacDonald, J. C. and Bernstein, J. (1990). Graph-set Analysis of Hydrogen-bond Patterns in Organic Crystals. **Acta Crystallogr., Sect. B: Struct. Sci.** 46: 256–262.
- Evans, K. E., Nkansah, M. A., Hutchinson, I. J. and Rogers, S. C. (1991). Molecular Network Design. **Nature** 353: 124–124.
- Fabian, J., Nakazumi, H. and Matsuoka, M. (1992). Near-infrared Absorbing Dyes. **Chem. Rev.** 92(6): 1197–1226.
- Fan, E., Vincent, C., Geib, S. J. and Hamilton, A. D. (1994). Molecular Recognition in the Solid State: Hydrogen-Bonding Control of Molecular Aggregation. **Chem. Mater.** 6: 1113–1117.
- Farrugia, L. J. (1997). *ORTEP-3* for Windows –A version of *ORTEP-III* with a graphical user interface (GUI). **J. Appl. Cryst.** 30: 565–565.
- Gavezzotti, A. (1996). Organic Crystals: Engineering and Design. **Current Opinion in Solid State & Material Science** 1: 501–505.
- Ghosh, K., Datta, M., Fröhlich, R. and Ganguly, N. C. (2005). Urotropine: a Unique Scaffold in Molecular Recognition for Phenolic Substrates. **J. Mol. Struct.** 733: 201–206.
- Glusker, J. P. and Trueblood, K. N. (1985). Crystal Structure Analysis: A Primer. 2nd Edition: Oxford University Press, Oxford.
- Hadebe, S. W., Robinson, R. S. and Munro, O. Q. (2007). A Bis(benzenedithiolate)-Bridged Dinuclear Rh^{III} Complex with Capping Triphenylphosphine Ligands

- and an Rh₂S₂ Core. **Acta Crystallogr., Sect. E: Struct. Rep. Online** 63: m175–m177.
- Herbstein, F. H., Dunitz, J. D. and Albert, J. A. (eds) (1971). Perspectives in Structural Chemistry. Wiley. New York.
- Kampermann, S. P., Ruble, J. R. and Craven, B. M. (1994). The Charge-density Distribution in Hexamethylenetetramine at 120 K. **Acta Crystallogr., Sect. B: Struct. Sci.** 50: 737–741.
- Karki, S., Friscic, T., Jones, W. and Motherwell W. D. S. (2007). Screening for Pharmaceutical Cocrystal Hydrates via Neat and Liquid-Assisted Grinding. **Mol. Pharm.** 4(3): 347–354.
- Kolotuchin, S V., Fenlon, E. E., Wilson, S. R., Loweth, C. J. and Zimmermann, S. C. (1995). Self-Assembly of 1,3,5-Benzenetricarboxylic Acids (Trimesic Acids) and Several Analogues in The Solid State. **Angew. Chem., Int. Ed. Engl.** 34(23): 2654–2657.
- Lehn, J.-M. (1995). Supramolecular Chemistry: Concepts and Perspectives. VCH, Weinheim.
- Lehn, J.-M., Atwood, J. L., Davies, J. E. D., MacNicol, D. D. and Vögtle, F. (eds) (1996). Comprehensive Supramolecular Chemistry. Pergamon Press, Oxford.
- Lommerse, J. P. M., Motherwell, W. D. S., Ammon, H. L., Dunitz, J. D., Gavezzotti, A., Hofmann, D. W. M., Leusen, F. J. J., Mooij, W. T. M., Price, S. L., Schweizer, B., Schmidt, M. U., van Eijck, B. P., Verwer, P. and Williams, D. E. (2000). A Test of Crystal Structure Prediction of Small Organic Molecules. **Acta Crystallogr., Sect. B: Struct. Sci.** 56: 697–714.

- MacLean, E. J., Glidewell, C., Ferguson, G., Gregson, R. M. and Lough, A. J. (1999). Hexamethylenetetramine is a Fourfold Acceptor of O–H···N Hydrogen Bonds in Its 1:2 Adduct with 2,2'-Biphenol. **Acta Crystallogr., Sect. C: Cryst. Struct. Commun.** 55(11): 1867–1870.
- MacNicol, D. D., McKendrick, J. J. and Wilson, D. R. (1978). Clathrates and Molecular Inclusion Phenomena. **Chem. Soc. Rev.** 7: 65–87.
- Mahmoud, M. M. and Wallwork, S. C. (1979). The Structures of the 1:1 Complexes Formed by Hexamethylenetetramine with Hydroquinone and Resorcinol. **Acta Crystallogr., Sect. B: Struct. Sci.** 35: 2370–2374.
- Motherwell, W. D. S., Ammon, H. M., Dunitz, J. D., Dzyabchenko, A., Erk, P., Gavezzotti, A., Hofmann, D. W. M., Leusen, F. J. J., Lommerse, J. P. M., Mooij, W. T. M., Price, S. L., Scheraga, H., Schweizer, B., Schmidt, M. U., van Eijck, B. P., Verwer, P. and Williams D. E. (2002). Crystal Structure Prediction of Small Organic Molecules: A Second Blind Test. **Acta Crystallogr., Sect. B: Struct. Sci.** 58: 647–661.
- Müller, P., Regine. H.-I., Spek, A., L., Schneider, T. R. and Sawaya, M. R. (2006). Crystal Structure Refinement: A Crystallographer's Guide to SHELXL. Oxford University Press, Oxford.
- Ng, S. W., Hu, S. Z., Hanna, J. V., Raj, S. S. S., Fun, H.-K., Razak, I. A., Wojciechowski, G. and Brzezinski, B.; (2001). X-Ray and Spectroscopic Re-Investigation of Urotropine–*p*-Nitrophenol Complex. **J. Mol. Struct.** 595: 189–194.
- Ng, S. W., Naumov, P., Ibrahim, A. R., Fun, H.-K., Chantapromma, S., Wojciechowski, G., Brzezinski, B. and Hanna, J. V. (2002). X-Ray and

- Spectroscopic Re-investigation of the 1:1 Complex Formed between Urotropine and Resorcinol. **J. Mol. Struct.** 609: 89–95.
- Oswald, I. D. H., Allan, D. R., McGregor, P. A., Motherwell, S. W. D., Parsons, S. and Pulham, C. R. (2002). The Formation of Paracetamol (Acetaminophen) Adducts with Hydrogen-Bond Acceptors. **Acta Crystallogr., Sect. B: Struct. Sci.** 58: 1057–1066.
- Oswald, I. D. H., Motherwell, S. W. D. and Parsons, S. (2005). Formations of Quinol Cocrystals with Hydrogen-Bond Acceptors. **Acta Crystallogr., Sect. B: Struct. Sci.** 61: 46–57.
- Pauling, L. (1960). The Nature of the Chemical Bond and the Structure of Molecules and Crystals: An Introduction to Modern Structural Chemistry, 3rd edition. Cornell University Press: Ithaca, NY.
- Phothikanith, A. (2003). Single Crystal X-Ray Characterization and Structure Correlation of Pentacyclic Friedelane Ring System. *Ph.D. Thesis*, Suranaree University of Technology, Nakhon Ratchasima 30000 Thailand.
- Phothikanith, A. and Haller, K. J. (2005). X-Ray Structural Characterization of Disordered Epifriedelin-3-ol and Friedelin-3-one. **Suranaree J. Sci. Tech.** 12(3): 211–222.
- Pinheiro C. B., Gardon M. and Chapuis G. (2003). Structural Changes of Hexamethylenetetramine and Undecanedioic Acid Cocrystal (HMT-C11) as a Function of the Temperature. **Acta Crystallogr., Sect. B: Struct. Sci.** 59: 416–427.
- Puntharod, R., Webster, G. T., Bambery, K. R., Asghari-Khiavi, M., Safinejad, F., Rivadeh, S., Langford, S., Haller, K. J. and Wood, B. R. (2010).

- Supramolecular Interactions Play an Integral Role in the Near-Infrared Raman "Excitonic" Enhancement Observed in Malaria Pigment and Other Related Heme Aggregates. **J. Phys. Chem. Sect. B** submitted for publication.
- Schmidt, G. M. J. (1971). Photodimerization in the Solid State. **Pure and Appl. Chem.** 27: 647–678.
- Shan, N., Bond, A. D. and Jones, W. (2002). Crystal Engineering Using 4,4'-Bipyridyl with Di- and Tricarboxylic Acids. 5: 9–24.
- Sheldrick, G. M. (1997). SHELXL-97: A Program for Crystal Structure Refinement. University of Göttingen, Germany.
- Sheth, A. R. and Grant, D. J. W. (2005). Relationship between the Structure and Properties of Pharmaceutical Crystals. **KONA** No.23 36–47.
- Shriver, D. F. and Drezzdon, M. A. (1986). The Manipulation of Air-Sensitive Compounds, 2nd Edition: J. Wiley and Sons, New York.
- Steed, J. W. and Atwood, J. L. (1995). Supramolecular Chemistry. VCH, Weinheim.
- Steiner, T. (2002). The Hydrogen Bonding in the Solid State. **Angew. Chem., Int. Ed.** 41(1): 48–76.
- Swamy, K. K. C., Kumaraswamy, S. and Kommana, P. (2001). Very Strong C–H \cdots O, N–H \cdots O, and O–H \cdots O Hydrogen Bonds Involving a Cyclic Phosphate. **J. Am. Chem. Soc.** 123: 12642–12649.
- Taylor, R. and Kennard, O. (1984). Hydrogen-Bond Geometry in Organic Crystals. **Acc. Chem. Res.** 17: 320–326.
- Trask, A. V., Motherwell, S. W. D. and Jones, W. (2004). Solvent-drop Grinding: Green Polymorph Control of Cocrystallization. **Chem. Commun.** 890–891.

- Trask, A. V., Motherwell, S. W. D. and Jones, W. (2006). Physical Stability Enhancement of Theophylline via Cocrystallization. **Int. J. Pharm.** 320: 114–123.
- Tremayne, M. and Glidewell, C. (2000). Direct-Space Structure Solution from Laboratory Powder Diffraction Data of an Organic Cocrystal: 1,2,3-Trihydroxybenzene–HMTA (1/1). **Chem. Commun.** 2425–2426.
- Tse, C., Wong, Y.-S. and Mak, T. C. W. (1977). Crystal Data for Some Molecular Complexes of Hexamethylenetetramine with Phenols. **J. Appl. Crystallogr.** 10: 68–69.
- Usman, A., Chantrapromma, S. and Fun, H.-K. (2001). Hexamethylenetetramine 2,4,6-trinitrophenolate. **Acta Crystallogr., Sect. C: Cryst. Struct. Commun.** 57: 1443–1446.
- Usman, A., Chantrapromma, S., Fun, H.-K., Poh, B.-L. and Karalia, C. (2002a). Hexamethylenetetramine 2,4,6-Trinitrophenolate. **Acta Crystallogr., Sect. C: Cryst. Struct. Commun.** 58(1): o46–o47.
- Usman, A., Chantrapromma, S., Fun, H.-K., Poh, B.-L. and Karalia, C. (2002b). A 1:1 adduct of hexamethylenetetramine and 4-Hydroxy-3-methoxy Benzaldehyde. **Acta Crystallogr., Sect. C: Cryst. Struct. Commun.** 58(1): o48–o50.
- Vishweshwar, P., McMahon, J. A., Bis, J. A. and Zaworotko, M. J. (2006). Pharmaceutical Co-Crystals. **J. Pharm. Sci.** 95(3): 499–516.
- Walsh, B. R. D., Bradner, M. W., Fleischman, S., Morales, L. A., Moulton, B., Hornedo, R. N. and Zaworotko, M. J. (2003). Crystal Engineering of the Composition of Pharmaceutical Phases. **Chem. Commun.** 186–187.

Wenger, M. and Bernstein, J. (2006). Designing a Cocrystal of γ -Amino Butyric Acid.

Angew. Chem., Int. Ed. Engl. 45: 7966–7969.

Wenger, M. and Bernstein, J. (2007). Cocrystal Design Gone Awry? A New

Dimorphic Hydrate of Oxalic Acid. **Mol. Pharm.** 4(3): 355–359.

Zakaria, C. M., Ferguson, G., Lough, A. J. and Glidewell, C. (2003). Adducts of

Hexamethylenetetramine with Ferrocenecarboxylic Acid and Ferrocene-1,1'-

Dicarboxylic Acid: Multiple Disorder in Space Groups *Fmm2* and *Cmcm*.

Acta Crystallogr., Sect. C: Cryst. Struct. Commun. 59(7): m271–m274.

APPENDICES

APPENDIX A

CRYSTALLIZATION

Crystallization procedures are often utilized for the final purification step in a synthesis or to obtain well formed or larger crystals required for single crystal X-ray diffraction or other techniques. In manufacturing crystallization is one objective accomplishment of a physical separation of a desired product from the mixture of other chemicals remaining from the synthesis. This stage of the synthesis is usually the final purification step used for the bulk substance and/or the removal of impurity.

A.1 Factors Affecting Crystallization

Several factors affect the size of the crystals during crystal growth, including the choice of solvent system, nucleation, and crystal growth conditions.

Solvent Selection

Generally selection of the right solvent system for a crystallization process is not specifically performance. Many factors must be considered as solubility, and reactivity are as important as their solvent property. Additional specifications might relate to toxicity and cost or even the versatility as a general laboratory solvent. Thus, water is frequently used as solvent for industrial crystallization when the chemical compound can be dissolved in water. Toxicity and cost of the solvent favor water, but other cost considerations may give the advantage to other solvents when the entire

process costs are considered. There are several organic liquids with good potential as crystallization solvents. They are usually divided into six groups: the lower alcohols and ketones, acetic acid and its esters, ethers, chlorinated hydrocarbons, benzene homologues, and light petroleum fractions. In many cases the solvent may already have been selected by the predominate process conditions.

Occasionally, a mixture of two or more solvents will be found to possess the best properties for a particular crystallization purpose. Common binary solvent mixtures that have proven useful include alcohols with water, ketones, ethers, chlorinated hydrocarbons or benzene homologues, *etc.* and normal alkanes with chlorinated hydrocarbons or aromatic hydrocarbons (Mullin, 2001). Sometimes, a second liquid is added to a solution to reduce the solubility of the solute to cause its precipitation/crystallization and at the same time maximize the yield of product. It is necessary for the two liquids (the original solvent and the added precipitant) to be miscible with one another. A common process of this type is the crystallization of an organic substance from water-miscible organic solvent by the controlled addition of water. The term ‘water-out’ is often used in this connection. This approach is also used to reduce the solubility of an inorganic salt in aqueous solution by the addition of less polar, water-miscible organic solvent to an aqueous solution.

Some of main points that should be considered when choosing a solvent for a crystallization process include the following. The solute to be crystallized should be readily soluble in the solvent. It should also be easily deposited from the solution in the desired crystalline form after cooling, evaporation, salting-out with an additive, *etc.* There are many exceptions to the frequently quoted rule that ‘like dissolves like’, but this rough empiricism can serve as a useful guide. Solvents may be classified as

being polar or nonpolar; the former description is given to liquids which have high dielectric constants, *e.g.* acids, alcohols, water, and the latter refers to liquids of low dielectric constant, *e.g.* aromatic hydrocarbons. A nonpolar solute (*e.g.* anthracene) is usually more soluble in a nonpolar solvent (*e.g.* benzene) than in a polar solvent (*e.g.* water). However, close chemical similarity between solute and solvent should be avoided, because their mutual solubility will in all probability be high, and crystallization may prove difficult or uneconomical. It should be noted that the crystal habit can often be changed by changing the solvent.

Based on the nature of their intermolecular bonding interactions solvents may be conveniently divided into three main classes: polar protic, *e.g.* water, methanol, acetic acid; dipolar aprotic, *e.g.* nitrobenzene, acetonitrile, furfural; and nonpolar aprotic, *e.g.* hexane, benzene, ethyl ether.

In polar protic solvents the solvent molecules interact by forming strong hydrogen bonds. In order to dissolve, the solute must break these bonds and replace them with bonds of similar strength. To have a reasonable solubility, therefore, the solute must be capable of forming hydrogen bonds, either because the solute itself is hydrogen bonded or because it is sufficiently strong Lewis base to accept a donated hydrogen atom to form a hydrogen bond. If the solute is aprotic and not basic it cannot form strong bonds with the solvent molecules and therefore will have a very low solubility.

In dipolar aprotic solvents, characterized by high dielectric constants, the solvent molecules interact by dipole–dipole interactions. If the solute is also dipolar and aprotic it can interact readily with the solvent molecules forming similar dipole–dipole interactions. If the solute is nonpolar it cannot interact with the dipoles of the

solvent molecules and so cannot dissolve. Protic solutes are found to be soluble in basic dipolar aprotic solvents because strong hydrogen bonds are formed, replacing the hydrogen bonds between the solute molecules in the solid state. If a dipolar aprotic solvent is not basic, however, a protic solute will have a low solubility because the strong hydrogen bonds in the solid phase can only be replaced by weaker dipole–dipole interactions between solvent and solute molecules.

In nonpolar aprotic solvents, characterized by low dielectric constants, molecules interact by weak van der Waals forces. Nonpolar solutes are readily soluble as the van der Waals forces between solute molecules in the solid phase are replaced by similar interactions with solvent molecules. Dipolar and polar protic solutes are generally found to have very low solubilities in these solvents except in cases where nonpolar complexes are formed.

The ‘power’ of a solvent is usually expressed as the mass of solute that can be dissolved in a given mass of pure solvent at one specified temperature. Water, for example, is a more powerful solvent at 20 °C for calcium chloride than n-propanol (75 and 16 g/100 g solvent). The temperature coefficient of solubility is another important factor to be considered when choosing a solvent for a cooling crystallization process in terms of quantity will influence the crystal yield. It frequently happens, especially in aqueous organic systems, that a low solubility is combined with a high temperature coefficient of solubility.

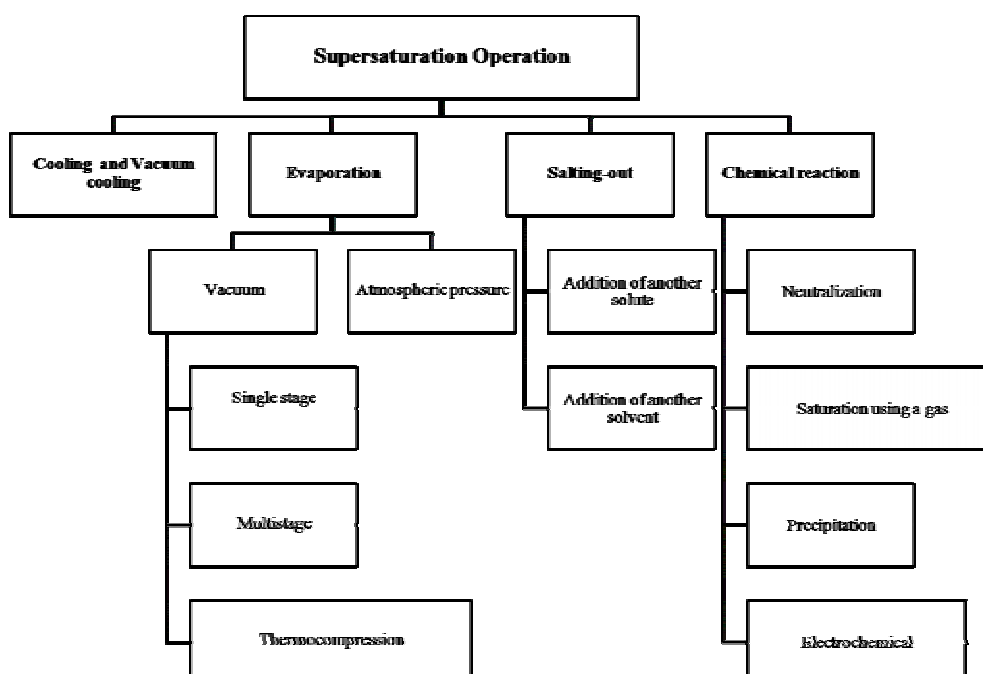
That dissolution rate of incomplete saturated solution in generally increases as temperature is raised. Then as the solution is allowed to cool, the solubility drops. Another method which may require hot solution is microscale when a minimum

amount of volatile solvents are used to fully dissolve a material, or when there is a low boiling point but also slow evaporation at normal temperatures.

Nucleation

In order for crystallization to take place a solution, a liquid, or a gas phase must be supersaturated and the required initiation step of homogeneous or heterogeneous nucleation that provides a small crystal form must take place. The nuclei then spontaneously grow crystals using driving forces which come from the different temperature and/or the concentration gradient created as Ohtaki has presented the process of formation of crystals from a supersaturated homogeneous solution as a nonequilibrium process.

Supersaturation can be created in several ways, some types of operations used are listed below:



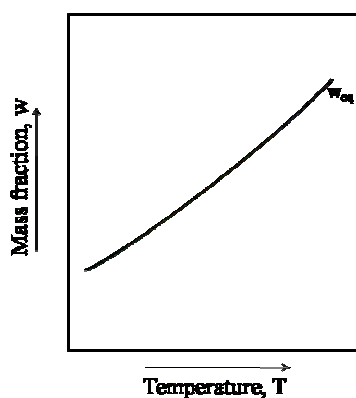


Figure A.1 Concentration diagram between mass fraction of crystallizing substance and temperature of the solution.

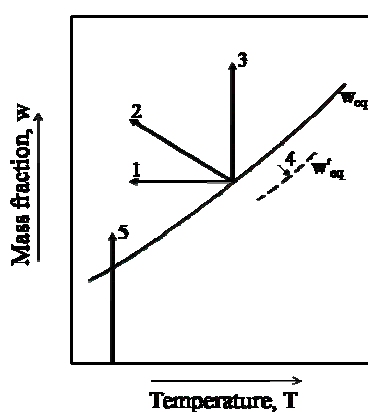


Figure A.2 Methods of supersaturation creation. 1, Cooling; 2, Vacuum cooling; 3, Isothermal evaporation; 4, Salting-out; 5, Chemical reaction.

A.2 Crystal Growth Techniques

Crystal growth is one common variety of purification that may be attempted. There are several different crystallization techniques that can be used.

Seeding

Crystallization requires an initiation step. This can be spontaneous or can be done by adding a small amount of the pure compound as seed crystals to the saturated

solution. Often initiation can be accomplished by simply scratching the glass surface to generate a seeding surface for crystal growth. It is also thought that dust particles can act as seeds initiators.

Solution Cooling

Typically a compound is dissolved in a minimum amount of solvent that fully dissolves the mixture *i.e.* create a saturated solution in the solute of interest. The solution is then allowed to cool. As the solution cools the solubility of the compounds in the solution drops, resulting in the desired compound dropping from solution. Generally, slower rates of cooling will yield fewer, and consequently larger crystals.

Slow Evaporation

In a typical slow evaporation experiment the compound is dissolved in a single suitable solvent and the solvent is allowed to slowly evaporate. Once the solution is saturated crystals can form. However, in the multi-solvent variation the solvent composition changes due to solvent composition changing as the more volatile solvent evaporates more quickly. The solvents are selected such that the compound has greater solubility in the more volatile solvent, and so the compound becomes increasingly insoluble in solution and the solution supersaturates and crystallizes.

Addition of a Second Solvent

A second solvent (often called the nonsolvent) is slowly added. The proportion of the two solvents is critical. Typically, the nonsolvent is added slowly until one of the compounds begins to crystallize from solution and the solution is then cooled to maximize the crystal yield. Heating is not required for this technique but can be used.

Vapor Diffusion

If a nonsolvent is more volatile than the solution solvent, the nonsolvent is allowed to evaporate from one container into another container holding the compound solution (vapor diffusion). As the solvent composition changes due to an increase in solvent that is has vapor diffusion into solution, the compound become increasingly insoluble in solution and crystallizes.

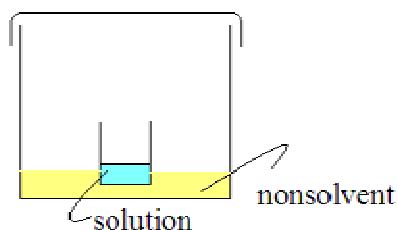


Figure A.3 Schematic drawing for vapor diffusion.

Liquid-liquid Diffusion

The less dense nonsolution solvent is filled into the rest tube, the two solvent mixed (often performed in an NMR tube) by liquid-liquid diffusion. A second solvent is layered carefully on the top of the solution containing the compound. Overtime the two solution mix, as the solvent composition changes due to diffusion, the compound becomes increasingly insoluble in solution and crystallizes, usually at the interface.

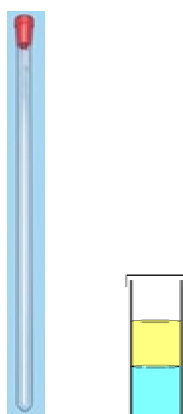


Figure A.4 NMR tubes and vials are often used for liquid-liquid diffusion.

Specialized equipment for liquid-liquid diffusion can also be in the shape of an “H-tube”, where one side arm of the H-tube is filled with a solution, then another additional solution or nonsolvent is filled into the opposite side arm.

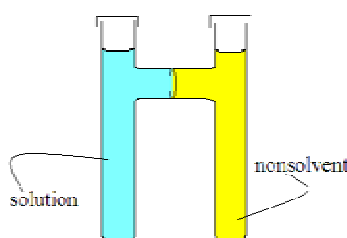


Figure A.5 H-tube apparatus.

Convection

A thermal gradient can be created in the crystal growing vessel using nichrome wire to provide local heating. When the heater is started solvent will start to circulate counterclockwise up the side tube. Cyclic current allows continual replenishing of solute. The solute will slowly saturate the solution. Material dissolves in the warm region and deposits in cool region as the solvent becomes saturated. The solvent will

be coolest at the bottom of the vertical tube where nucleation and crystal growth can occur. The velocity of convection current is proportional to the magnitude of the thermal gradient.

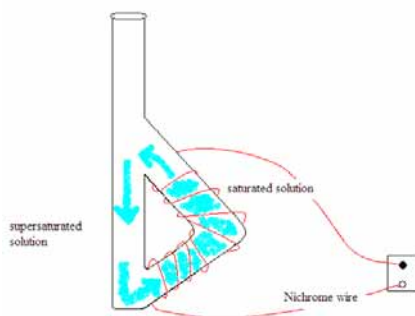


Figure A.6 Thiele tube apparatus.

Sublimation

Gas to solid phase crystal growth of compounds with appreciable solid phase vapour pressure and good thermal stability can be performed using a vacuum sealed tube placed in an oven or tube furnace for several days or even weeks. Various means can be employed to slow the process, such as adding packed materials in the tube followed by glass wool. The tube can be placed under active or static vacuum and/or a thermal gradient can be established by heating the loaded end of the tube, for example by placing a copper pipe around the tube. Specially sublimation glassware available as show below.

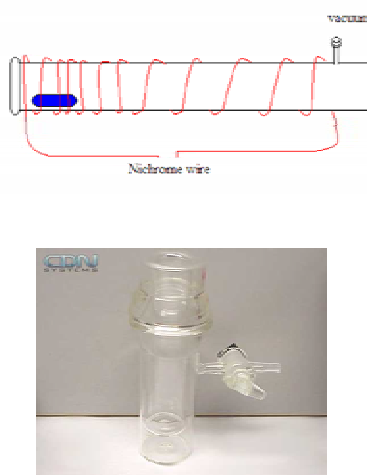


Figure A.7 Sublimation apparatus.

Recrystallization

The optimum size for a crystal for a single crystal X-Ray structure determination is one which has dimensions of approximately 0.2-0.4 mm in at least two of the three dimensions. Crystals obtained from reactions are often finer precipitates so must be recrystallized to obtain suitable size. Precipitation is sometimes a relatively fast process and occurs in minutes or hours, so impurities in the solution are often trapped as the precipitate forms with resulting impure crystals. The impurities may affect the size and quality of a single crystal. The crystallization process is slow compared to precipitation techniques and requires relatively long periods of time (days to weeks) to ensure that no impurities will be trapped in the crystal lattice as the crystal grows. Thus, a solid is often simultaneously purified as a size suitable for single crystal X-ray diffraction is formed by recrystallization techniques as described above.

A.3 Cocrystallization

In practice, however, there are challenges in screening for cocrystals and their subsequent scaling-up. Currently, various techniques are employed to prepare cocrystals including slow evaporation, slurrying of suspensions, crystallization by cooling, and the co-grinding method.

Crystallization by Cooling

Slow cooling of cocrystal components from solution remains the most industrially-preferred process, even though there is some risk of crystallizing the single component phase. Thus, numerous experimental conditions have to be tested in the laboratory, and scaling-up the crystallization process remains a challenge. To this end isothermal phase diagrams of cocrystal-forming systems are very useful in reducing the number of experiments and can help explain the success rate of solvent drop-grinding experiments.

Co-grinding Method

Co-grinding method involves mixing two solids together in a mill, optionally with a very small amount of solvent (solvent drop grinding), to induce cocrystal formation through mechanochemistry. Although this is recognized as one of the most efficient methods for preparing cocrystals, scaling-up is not always obvious.

APPENDIX B

AIR-SENSITIVE TECHNIQUES

Shriver and Drezdson (1986) have presented an excellent description of the more complicated techniques used to manipulate air-sensitive organic, inorganic, organometallic, and biochemical materials with the exclusion of air. Schlenk techniques refer to a series of common techniques to perform operations on air-sensitive materials in the absence of a glove box.

Manifolds for medium vacuum to gas from the equipment and for introducing an inert gas are key parts of the Schlenk line setup. When economy is the primary concern nitrogen is the inert gas of choice. If nitrogen might react with the system under study the noble gases, argon or helium may be used. Argon may also be used if it is desirable that the inert atmosphere be denser than oxygen.

When the pump-and-fill technique is to be used, a more complex manifold for the distribution in conjunction with a liquid nitrogen-cooled trap, a mechanical vacuum pump, and pressure release bubblers is employed.

This manifold can be used to purge several pieces of apparatus at once, and the two-way stopcocks or valves provide a ready means of switching between inert gas and vacuum. The liquid nitrogen-cooled trap is used to protect the rotary mechanical vacuum pump from chemicals and solvent vapor. **CAUTION: A liquid nitrogen trap must never be connected to a manifold where the vacuum source**

has been turned off. Failure to remove a liquid nitrogen trap from a manifold after shutting off the vacuum will result in the condensation of liquid air in trap. If warmed, this liquid air will evaporate and may pressurize the apparatus, presenting an extreme explosion hazard. In general a high vacuum is not required for pump-and-fill types of purge used in Schlenk techniques. Several cycles of pumping and filling with inert gas are sufficient in each step it is important to reduce the oxygen and other atmospheric gases to very low level on the system.

Reaction vessels are available in a variety of shapes and sizes. Schlenk flasks are simply round-bottom or pear-shaped flasks that have a stopcock or valve attached to them as a sidearm through which the air in the apparatus can be evacuated or the apparatus can be filled with inert gas. Schlenk tubes are round-bottom glass cylinders with a sidearm near the top. Schlenk ware permits the transfer of liquids or solids by pouring within a closed apparatus or under an inert-gas flush. Furthermore, the sidearm provides several alternatives to maintain a constant flush of inert gas on the solid transfer vessel when it is attached to another piece of apparatus in any system that air can not enter. Since it is possible to perform fairly complex solids transfer operations with this type of apparatus, the need for glove box operations is minimized.

Some of the basic items of equipment include a Schlenk tube (which is used as a reaction flask), a fritted funnel, a dropping funnel, and a solids container. The ground glass joint is used to connect the flask to other apparatus or is plugged with a stopper or rubber septum. The stopcocks are made out of glass or Teflon, the latter being preferred because they are easier to clean and won't leach grease into the reaction mixture.

Schlenk technique is an indispensable tool for manipulating air-sensitive materials when incorporated with other techniques such as syringe techniques or cannula transfer techniques using rubber septa with needles to transfer or to mix additional individual liquid reagents and solutions from one flask to another while excluding air. A cannula is essentially a needle, where one or both ends are sharpened. The solution is forced through the needle or cannula by means of the pressure differential that is achieved via vacuum and relative inert gas pressure.

Counterflow is created by opening the sidearm valve inlet and turning up the inert gas flow, then holding on to the stopper. Remove the stopper from the flask and nitrogen will flow in through the sidearm and out the joint, protecting the contents from air and water. Place the addition funnel on the flask and allow the apparatus to purge completely with nitrogen. Place a stopper in the top of the addition funnel and reduce the nitrogen pressure on the manifold. Leave the sidearm valve open to the nitrogen manifold and bubbler. Adjust the nitrogen flow so that the bubbler bubbles once every few seconds.

The solvent is often present in large excess over most reagents. It is important to achieve a low level of reactive impurity in the solvent. Purging solvents with inert gas is one common method used to remove oxygen from solvents prior to setting up the reaction. This method works well with saturated aliphatic, aromatic, and chlorinated hydrocarbons.

APPENDIX C

CRYSTALLOGRAPHIC INFORMATION FILE FOR

[*o*-C₆H₄(OH)₂]:[(CH₂)₆N₄]

data_ks

_audit_creation_method	SHELXL-97
_chemical_name_systematic	
;	
?	
;	
_chemical_name_common	hexamine-catechol
_chemical_melting_point	?
_chemical_formula_moiety	C6 H12 N4, 2(C6 H6 O2)
_chemical_formula_sum	C18 H24 N4 O4
_chemical_formula_weight	360.41

loop_

_atom_type_symbol	
_atom_type_description	
_atom_type_scatter_dispersion_real	
_atom_type_scatter_dispersion_imag	
_atom_type_scatter_source	
'C'	'C' 0.0033 0.0016
'International Tables Vol C Tables 4.2.6.8 and 6.1.1.4'	
'H'	'H' 0.0000 0.0000
'International Tables Vol C Tables 4.2.6.8 and 6.1.1.4'	
'N'	'N' 0.0061 0.0033
'International Tables Vol C Tables 4.2.6.8 and 6.1.1.4'	
'O'	'O' 0.0106 0.0060
'International Tables Vol C Tables 4.2.6.8 and 6.1.1.4'	

_symmetry_cell_setting	?
_symmetry_space_group_name_H-M	?

loop_

_symmetry_equiv_pos_as_xyz	
'x, y, z'	
'-x, y, -z+1/2'	
'x+1/2, y+1/2, z'	
'-x+1/2, y+1/2, -z+1/2'	
'-x, -y, -z'	
'x, -y, z-1/2'	
'-x+1/2, -y+1/2, -z'	
'x+1/2, -y+1/2, z-1/2'	

_cell_length_a	23.5925(7)
_cell_length_b	6.8339(2)
_cell_length_c	13.1856(3)
_cell_angle_alpha	90.00
_cell_angle_beta	123.1362(17)
_cell_angle_gamma	90.00
_cell_volume	1780.17(8)
_cell_formula_units_Z	4
_cell_measurement_temperature	200(2)
_cell_measurement_reflns_used	?
_cell_measurement_theta_min	?
_cell_measurement_theta_max	?
_exptl_crystal_description	?
_exptl_crystal_colour	?
_exptl_crystal_size_max	0.48
_exptl_crystal_size_mid	0.37
_exptl_crystal_size_min	0.35
_exptl_crystal_density_meas	?
_exptl_crystal_density_diffn	1.345
_exptl_crystal_density_method	'not measured'
_exptl_crystal_F_000	768
_exptl_absorpt_coefficient_mu	0.097
_exptl_absorpt_correction_type	?
_exptl_absorpt_correction_T_min	0.9551
_exptl_absorpt_correction_T_max	0.9669
_exptl_absorpt_process_details	?
_exptl_special_details	
;	
?	
;	
_diffn_ambient_temperature	200(2)
_diffn_radiation_wavelength	0.71073
_diffn_radiation_type	MoK\alpha
_diffn_radiation_source	'fine-focus sealed tube'
_diffn_radiation_monochromator	graphite
_diffn_measurement_device_type	?
_diffn_measurement_method	?
_diffn_detector_area_resol_mean	?
_diffn_standards_number	?
_diffn_standards_interval_count	?
_diffn_standards_interval_time	?
_diffn_standards_decay_%	?
_diffn_reflns_number	2260
_diffn_reflns_av_R_equivalents	0.0000
_diffn_reflns_av_sigmaI/netI	0.0249
_diffn_reflns_limit_h_min	0
_diffn_reflns_limit_h_max	31
_diffn_reflns_limit_k_min	0
_diffn_reflns_limit_k_max	9
_diffn_reflns_limit_l_min	-17
_diffn_reflns_limit_l_max	14
_diffn_reflns_theta_min	5.12
_diffn_reflns_theta_max	28.73

```

_reflns_number_total      2260
_reflns_number_gt         1952
_reflns_threshold_expression >2sigma(I)

_computing_data_collection ?
_computing_cell_refinement ?
_computing_data_reduction ?
_computing_structure_solution 'SHELXS-97 (Sheldrick, 1990)'
_computing_structure_refinement 'SHELXL-97 (Sheldrick, 1997)'
_computing_molecular_graphics ?
_computing_publication_material ?

_refine_special_details
;
  Refinement of F2 against ALL reflections. The weighted R-
  factor wR and
  goodness of fit S are based on F2, conventional R-factors R
  are based
  on F, with F set to zero for negative F2. The threshold
  expression of
  F2 > 2sigma(F2) is used only for calculating R-factors(gt)
  etc. and is
  not relevant to the choice of reflections for refinement. R-
  factors based
  on F2 are statistically about twice as large as those based on
  F, and R-
  factors based on ALL data will be even larger.
;

_refine_ls_structure_factor_coef Fsqd
_refine_ls_matrix_type full
_refine_ls_weighting_scheme calc
_refine_ls_weighting_details
'calc w=1/[\s2(Fo2)+(0.0442P)2+1.1619P] where
P=(Fo2+2Fc2)/3'
_refine_ls_solution_primary direct
_refine_ls_solution_secondary difmap
_refine_ls_solution_hydrogens geom
_refine_ls_hydrogen_treatment mixed
_refine_ls_extinction_method none
_refine_ls_extinction_coef ?
_refine_ls_number_reflns 2260
_refine_ls_number_parameters 173
_refine_ls_number_restraints 0
_refine_ls_R_factor_all 0.0605
_refine_ls_R_factor_gt 0.0457
_refine_ls_wR_factor_ref 0.1155
_refine_ls_wR_factor_gt 0.1003
_refine_ls_goodness_of_fit_ref 1.174
_refine_ls_restrained_S_all 1.174
_refine_ls_shift/su_max 0.005
_refine_ls_shift/su_mean 0.001

loop_
  _atom_site_label
  _atom_site_type_symbol
  _atom_site_fract_x

```

```

_atom_site_fract_y
_atom_site_fract_z
_atom_site_U_iso_or_equiv
_atom_site_adp_type
_atom_site_occupancy
_atom_site_symmetry_multiplicity
_atom_site_calc_flag
_atom_site_refinement_flags
_atom_site_disorder_assembly
_atom_site_disorder_group
C1 C 0.65080(7) 0.0441(2) 0.65433(12) 0.0281(3) Uani 1 1 d . . .
O1 O 0.61449(6) 0.06386(17) 0.53123(9) 0.0402(3) Uani 1 1 d . . .
H1 H 0.5877(13) -0.047(4) 0.487(2) 0.078(7) Uiso 1 1 d . . .
C2 C 0.63788(6) -0.1068(2) 0.71033(12) 0.0274(3) Uani 1 1 d . . .
O2 O 0.58789(5) -0.23533(16) 0.63584(9) 0.0396(3) Uani 1 1 d . .
.
H2 H 0.5828(11) -0.337(3) 0.682(2) 0.071(7) Uiso 1 1 d . . .
C3 C 0.67483(7) -0.1193(2) 0.83560(12) 0.0309(3) Uani 1 1 d . . .
H3 H 0.6644(8) -0.227(3) 0.8728(15) 0.038(4) Uiso 1 1 d . . .
C4 C 0.72583(7) 0.0150(2) 0.90581(13) 0.0346(3) Uani 1 1 d . . .
H4 H 0.7514(10) 0.005(3) 0.9950(18) 0.047(5) Uiso 1 1 d . . .
C5 C 0.73926(7) 0.1627(2) 0.85059(14) 0.0368(3) Uani 1 1 d . . .
H5 H 0.7760(10) 0.258(3) 0.8996(18) 0.052(5) Uiso 1 1 d . . .
C6 C 0.70166(8) 0.1785(2) 0.72511(14) 0.0351(3) Uani 1 1 d . . .
H6 H 0.7095(9) 0.283(3) 0.6826(16) 0.046(5) Uiso 1 1 d . . .
C7 C 0.5000 0.1138(3) 0.7500 0.0268(4) Uani 1 2 d S . .
H7 H 0.4692(7) 0.029(2) 0.7623(13) 0.025(4) Uiso 1 1 d . . .
N1 N 0.45847(5) 0.23372(16) 0.64058(9) 0.0253(3) Uani 1 1 d . . .
C8 C 0.50405(7) 0.3598(2) 0.62595(12) 0.0276(3) Uani 1 1 d . . .
H8A H 0.5348(8) 0.274(2) 0.6147(15) 0.034(4) Uiso 1 1 d . . .
H8B H 0.4759(8) 0.442(2) 0.5525(14) 0.030(4) Uiso 1 1 d . . .
C9 C 0.58571(6) 0.3594(2) 0.84044(12) 0.0284(3) Uani 1 1 d . . .
H9A H 0.6127(8) 0.440(2) 0.9154(15) 0.034(4) Uiso 1 1 d . . .
H9B H 0.6171(8) 0.276(3) 0.8290(15) 0.036(4) Uiso 1 1 d . . .
N2 N 0.54607(6) 0.48585(16) 0.73289(10) 0.0267(3) Uani 1 1 d . .
.
C10 C 0.5000 0.6063(3) 0.7500 0.0291(4) Uani 1 2 d S . .
H10 H 0.4731(8) 0.691(2) 0.6762(14) 0.035(4) Uiso 1 1 d . . .

loop_
_atom_site_aniso_label
_atom_site_aniso_U_11
_atom_site_aniso_U_22
_atom_site_aniso_U_33
_atom_site_aniso_U_23
_atom_site_aniso_U_13
_atom_site_aniso_U_12
C1 0.0321(6) 0.0281(7) 0.0283(6) -0.0037(5) 0.0192(6) -0.0040(5)
O1 0.0553(7) 0.0361(6) 0.0276(5) -0.0033(4) 0.0217(5) -0.0168(5)
C2 0.0267(6) 0.0279(7) 0.0286(6) -0.0039(5) 0.0158(5) -0.0048(5)
O2 0.0452(6) 0.0397(6) 0.0269(5) -0.0031(4) 0.0152(5) -0.0217(5)
C3 0.0318(7) 0.0333(7) 0.0285(7) -0.0005(5) 0.0170(6) -0.0002(6)
C4 0.0302(7) 0.0407(8) 0.0287(7) -0.0072(6) 0.0134(6) 0.0001(6)
C5 0.0323(7) 0.0385(8) 0.0388(8) -0.0147(6) 0.0190(6) -0.0101(6)
C6 0.0397(7) 0.0322(7) 0.0410(8) -0.0083(6) 0.0269(7) -0.0113(6)
C7 0.0340(9) 0.0199(8) 0.0308(9) 0.000 0.0204(8) 0.000
N1 0.0296(5) 0.0224(5) 0.0249(5) -0.0024(4) 0.0154(4) -0.0045(4)

```

```

C8 0.0349(7) 0.0259(6) 0.0252(6) -0.0027(5) 0.0185(6) -0.0055(5)
C9 0.0247(6) 0.0296(7) 0.0270(6) 0.0005(5) 0.0116(5) 0.0002(5)
N2 0.0301(5) 0.0237(5) 0.0262(5) -0.0012(4) 0.0153(5) -0.0050(4)
C10 0.0367(10) 0.0178(8) 0.0293(9) 0.000 0.0158(8) 0.000

_geom_special_details
;
  All esds (except the esd in the dihedral angle between two l.s.
  planes)
  are estimated using the full covariance matrix. The cell esds
  are taken
  into account individually in the estimation of esds in
  distances, angles
  and torsion angles; correlations between esds in cell parameters
  are only
  used when they are defined by crystal symmetry. An approximate
  (isotropic)
  treatment of cell esds is used for estimating esds involving
  l.s. planes.
;

loop_
  _geom_bond_atom_site_label_1
  _geom_bond_atom_site_label_2
  _geom_bond_distance
  _geom_bond_site_symmetry_2
  _geom_bond_publ_flag
C1 O1 1.3661(16) 1 ?
C1 O1 1.3661(16) . ?
C1 C6 1.3890(19) . ?
C1 C2 1.3959(19) . ?
O1 O1 0.000(3) 1 ?
O1 H1 0.95(3) . ?
C2 O2 1.3641(16) 1 ?
C2 O2 1.3641(16) . ?
C2 C3 1.3862(18) . ?
O2 O2 0.000(4) 1 ?
O2 H2 0.98(2) . ?
C3 C4 1.389(2) . ?
C3 H3 0.987(18) . ?
C4 C5 1.379(2) . ?
C4 H4 0.988(19) . ?
C5 C6 1.390(2) . ?
C5 H5 0.99(2) . ?
C6 H6 0.984(19) . ?
C7 N1 1.4725(14) 2_656 ?
C7 N1 1.4725(14) . ?
C7 H7 1.008(15) . ?
N1 C8 1.4707(16) . ?
N1 C9 1.4740(17) 2_656 ?
C8 N2 1.4781(16) . ?
C8 H8A 1.007(17) . ?
C8 H8B 0.995(16) . ?
C9 N1 1.4740(17) 2_656 ?
C9 N2 1.4772(16) . ?
C9 H9A 0.998(17) . ?
C9 H9B 1.010(17) . ?

```

```

N2 C10 1.4758(15) . ?
C10 N2 1.4758(15) 2_656 ?
C10 H10 1.004(16) . ?

loop_
  _geom_angle_atom_site_label_1
  _geom_angle_atom_site_label_2
  _geom_angle_atom_site_label_3
  _geom_angle
  _geom_angle_site_symmetry_1
  _geom_angle_site_symmetry_3
  _geom_angle_publ_flag
O1 C1 O1 0.0 1 . ?
O1 C1 C6 118.91(12) 1 . ?
O1 C1 C6 118.91(12) . . ?
O1 C1 C2 121.66(12) 1 . ?
O1 C1 C2 121.66(12) . . ?
C6 C1 C2 119.42(13) . . ?
O1 O1 C1 0(10) 1 . ?
O1 O1 H1 0(10) 1 . ?
C1 O1 H1 115.2(14) . . ?
O2 C2 O2 0.00(11) 1 . ?
O2 C2 C3 123.46(12) 1 . ?
O2 C2 C3 123.46(12) . . ?
O2 C2 C1 116.61(12) 1 . ?
O2 C2 C1 116.61(12) . . ?
C3 C2 C1 119.93(12) . . ?
O2 O2 C2 0(10) 1 . ?
O2 O2 H2 0(10) 1 . ?
C2 O2 H2 111.1(13) . . ?
C2 C3 C4 120.33(13) . . ?
C2 C3 H3 118.2(10) . . ?
C4 C3 H3 121.4(10) . . ?
C5 C4 C3 119.80(13) . . ?
C5 C4 H4 120.9(12) . . ?
C3 C4 H4 119.3(12) . . ?
C4 C5 C6 120.28(13) . . ?
C4 C5 H5 120.7(11) . . ?
C6 C5 H5 119.1(11) . . ?
C1 C6 C5 120.22(14) . . ?
C1 C6 H6 117.2(11) . . ?
C5 C6 H6 122.6(11) . . ?
N1 C7 N1 112.34(14) 2_656 . ?
N1 C7 H7 108.2(8) 2_656 . ?
N1 C7 H7 108.9(8) . . ?
C8 N1 C7 108.19(9) . . ?
C8 N1 C9 108.44(10) . 2_656 ?
C7 N1 C9 108.16(9) . 2_656 ?
N1 C8 N2 111.93(10) . . ?
N1 C8 H8A 108.2(9) . . ?
N2 C8 H8A 108.7(9) . . ?
N1 C8 H8B 108.1(9) . . ?
N2 C8 H8B 110.0(9) . . ?
H8A C8 H8B 109.8(13) . . ?
N1 C9 N2 111.62(10) 2_656 . ?
N1 C9 H9A 106.3(9) 2_656 . ?
N2 C9 H9A 110.8(10) . . ?

```

```

N1 C9 H9B 109.9(10) 2_656 . ?
N2 C9 H9B 108.6(9) . . ?
H9A C9 H9B 109.6(13) . . ?
C10 N2 C9 108.19(9) . . ?
C10 N2 C8 107.75(9) . . ?
C9 N2 C8 108.52(10) . . ?
N2 C10 N2 112.19(14) . 2_656 ?
N2 C10 H10 107.5(9) . . ?
N2 C10 H10 109.9(9) 2_656 . ?

loop_
  _geom_torsion_atom_site_label_1
  _geom_torsion_atom_site_label_2
  _geom_torsion_atom_site_label_3
  _geom_torsion_atom_site_label_4
  _geom_torsion
  _geom_torsion_site_symmetry_1
  _geom_torsion_site_symmetry_2
  _geom_torsion_site_symmetry_3
  _geom_torsion_site_symmetry_4
  _geom_torsion_publ_flag
C6 C1 O1 O1 0.0(2) . . . 1 ?
C2 C1 O1 O1 0.00(19) . . . 1 ?
O1 C1 C2 O2 1.0(2) 1 . . 1 ?
O1 C1 C2 O2 1.0(2) . . . 1 ?
C6 C1 C2 O2 -179.21(13) . . . 1 ?
O1 C1 C2 O2 1.0(2) 1 . . . ?
O1 C1 C2 O2 1.0(2) . . . . ?
C6 C1 C2 O2 -179.21(13) . . . . ?
O1 C1 C2 C3 -178.56(13) 1 . . . ?
O1 C1 C2 C3 -178.56(13) . . . . ?
C6 C1 C2 C3 1.2(2) . . . . ?
C3 C2 O2 O2 0.00(4) . . . 1 ?
C1 C2 O2 O2 0.00(8) . . . 1 ?
O2 C2 C3 C4 178.91(13) 1 . . . ?
O2 C2 C3 C4 178.91(13) . . . . ?
C1 C2 C3 C4 -1.6(2) . . . . ?
C2 C3 C4 C5 0.7(2) . . . . ?
C3 C4 C5 C6 0.5(2) . . . . ?
O1 C1 C6 C5 179.72(13) 1 . . . ?
O1 C1 C6 C5 179.72(13) . . . . ?
C2 C1 C6 C5 -0.1(2) . . . . ?
C4 C5 C6 C1 -0.8(2) . . . . ?
N1 C7 N1 C8 58.51(7) 2_656 . . . ?
N1 C7 N1 C9 -58.76(7) 2_656 . . 2_656 ?
C7 N1 C8 N2 -57.99(14) . . . . ?
C9 N1 C8 N2 59.10(13) 2_656 . . . ?
N1 C9 N2 C10 58.29(13) 2_656 . . . ?
N1 C9 N2 C8 -58.35(14) 2_656 . . . ?
N1 C8 N2 C10 -58.67(13) . . . . ?
N1 C8 N2 C9 58.26(14) . . . . ?
C9 N2 C10 N2 -58.61(8) . . . 2_656 ?
C8 N2 C10 N2 58.53(7) . . . 2_656 ?

loop_
  _geom_hbond_atom_site_label_D
  _geom_hbond_atom_site_label_H

```

```

_geom_hbond_atom_site_label_A
_geom_hbond_distance_DH
_geom_hbond_distance_HA
_geom_hbond_distance_DA
_geom_hbond_angle_DHA
_geom_hbond_site_symmetry_A
O1 H1 N1  0.95(3) 1.91(3) 2.8227(15) 160(2) 5_656
O2 H2 N2  0.98(2) 1.81(2) 2.7608(15) 162(2) 1_545
O1 H1 O2  0.95(3) 2.35(2) 2.7246(14) 103.0(16) 1
C7 H7 O2  1.008(15) 2.978(15) 3.9584(16) 164.6(11) 2_656
C7 H7 O1  1.008(15) 3.306(14) 3.4015(12) 86.8(8) 5_656
C7 H7 C10  1.008(15) 3.006(15) 3.468(3) 109.0(10) 1_545
C8 H8A O1  1.007(17) 3.010(17) 3.9997(18) 167.7(12) 1
C8 H8B O2  0.995(16) 2.518(15) 3.0263(16) 111.4(11) 5_656
C10 H10 O1  1.004(16) 2.895(16) 3.8958(15) 174.5(12) 5_666
C10 H10 C7  1.004(16) 3.006(17) 3.468(3) 109.2(11) 1_565

_diffn_measured_fraction_theta_max    0.979
_diffn_reflns_theta_full              28.73
_diffn_measured_fraction_theta_full    0.979
_refine_diff_density_max               0.199
_refine_diff_density_min              -0.247
_refine_diff_density_rms              0.044

```


APPENDIX D

SUPPORTING INFORMATION FOR CHAPTER IV

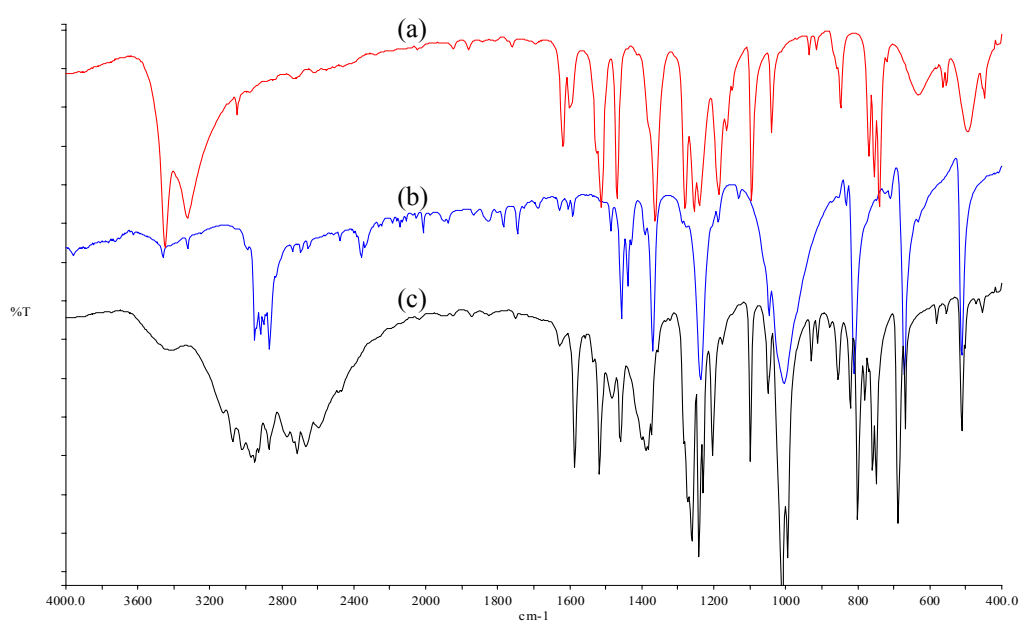


Figure D.1 Infrared spectra of (a) catechol, (b) hexamine, and (c) catechol–hexamine.

APPENDIX E

LIST OF PRESENTATIONS

1. **Kadsada Sala**, Kenneth J. Haller, Seik Weng Ng (2006). Crystal Structure of 2:1 Adduct of 1,2-Benzenediol and Hexamethylenetetramine. *The 2006 Meeting of the American Crystallographic Association*, Honolulu, Hawaii, USA, July 22–26.
2. **Kadsada Sala**, Kenneth J. Haller, Seik Weng Ng (2006). Supramolecular Structure of Cocrystallized Catechol and Hexamine. *Joint Conference of the Asian Crystallographic Association and the Crystallographic Society of Japan*, Tsukuba, Japan, November 20–23.
3. Navarat Sodesiri, Oratai Saisa-ard, **Kadsada Sala**, Kenneth J. Haller (2007) Synthesis and Physical Characterization of an Ethylenediamine and Cyanuric Acid Cocrystal. *The 33rd Congress on Science and Technology of Thailand 2007*, Nakhon Sri Thammarat, Thailand, October 18–20.
4. **Kadsada Sala**, Kenneth J. Haller (2009). Supramolecular Structure of Cocrystallized Catechol and Hexamine. *The German-Thai Symposium on Nanoscience and Nanotechnology*, Chaing Mai, Thailand, September 21–22.

CURRICULUM VITAE

Name: Miss Kadsada Sala

Date of Birth: 27 May 1983

Place of Birth: Loei, Thailand

Citizenship: Thai

Education:

2005 B. Sc. (Chemistry) Maejo University, Chiang Mai, Thailand

2010 M. Sc. (Chemistry) Suranaree University of Technology,
Nakhon Ratchasima, Thailand

Relevant Experience:

2006–2009 Teaching Assistant, School of Chemistry, Institute of Science,
Suranaree University of Technology

Scholarships, Grant, and Fellowships:

2006 American Crystallographic Association Travel Grant

2006–2010 Teaching Assistant, Suranaree University of Technology

2007–2008 SUT Scholarship